CHARACTERIZATION OF NONHUMAN PRIMATE LUNG AND BRONCHOALVEOLAR LAVAGE SAMPLES BY FLOW CYTOMETRY FOLLOWING AEROSOL CHALLENGE WITH VIRAL PATHOGENS

by

Abigail Bowlsbey Lara

B.A. (Hood College) 1999

THESIS

Submitted in partial satisfaction of the requirements

for the degree of

MASTER OF SCIENCE

in

BIOMEDICAL SCIENCE

in the

GRADUATE SCHOOL

of

HOOD COLLEGE

Fall 2018

Accepted:

_____	_____
Ricky Hirschhorn, Ph.D	Ann Boyd, Ph.D
Committee Member	Director, Biomedical Science Program
_____	_____
Jeffrey Rossio, Ph.D.	April Boulton, PhD
Committee Member	Dean of Graduate School
_____	
Michael Holbrook, Ph.D.	
Thesis Adviser	

STATEMENT OF USE AND COPYRIGHT WAIVER

I authorize Hood College to lend this thesis, or reproductions of it, in total or part, at the request of other institutions or individuals for the purpose of scholarly research.

TABLE OF CONTENTS

	Page
ABSTRACT	vi
LIST OF TABLES	viii
LIST OF FIGURES	ix
LIST OF ABBREVIATIONS	xi
INTRODUCTION	1
Background	1
Rationale	3
Objectives	6
MATERIALS AND METHODS	9
Panel Design	9
Tissue Collection	14
Tissue Processing	15
Staining for Flow Cytometry	16
Fluorescence Minus One (FMO) controls	17
Anti-Nipah Polyclonal Antibody Development, Purification, and Labeling	17
Mouse anti-EBOV VP40 Antibody Labeling	18

Data Analysis 18

RESULTS 19

Objective I - Comparison of panel to published data for rhesus 19

Objective II - Determination of normal values for African Green monkeys 23

Objective III - Comparison of normal rhesus lung samples to Ebola-infected samples 28

Objective IV - Comparison of normal AGM samples to Nipah-infected samples 34

DISCUSSION 45

Objective I - Comparison of panel to published data for rhesus 45

Objective II - Determination of normal values for African Green monkeys (AGM) 47

Objective III - Comparison of normal rhesus lung samples to Ebola-infected samples 49

Objective IV - Comparison of normal AGM samples to Nipah-infected samples 52

Conclusions 53

REFERENCES 55

ABSTRACT

Outbreaks of several highly pathogenic viruses such as Ebola virus, Marburg virus, and Nipah virus occur periodically in some parts of the world. Because these viruses are highly infectious and associated with high mortality rates, there is some concern that one or more of them could be developed as a bioweapon. In order to be able to effectively treat victims of outbreaks as well as understand and counter the possibility of one of these agents being used in an act of bioterrorism, they are studied extensively in specialized labs throughout the world.

Nonhuman primates are frequently used as models in the study of high consequence viral pathogens because of their similarity to humans. Typically, a nonhuman primate species is selected as a model for each virus based on similarity of disease course to that in humans. In addition to species selection, a challenge route must be selected according to the specific goals of the proposed study. In spite of there not having ever been a documented case of a human contracting any of these viruses via aerosol transmission, aerosol challenge is common in these types of studies due to concerns that one of these viruses could be altered in some way, as a bioterrorism agent, that would allow it to infect via aerosols.

Since the lungs are the primary challenge site in an aerosol infection, valuable information could be gleaned from monitoring changes in the lungs. Unfortunately, there is a scarcity in the published literature of information about the normal lung environment in nonhuman primate (NHP) species. In order to determine abnormalities that occur due to infection and pathogenesis it is important to first determine what that environment typically looks like in a normal uninfected individual of the same species.

In this work, the lung environment in normal rhesus macaques and African Green monkeys was characterized through the use of flow cytometric analysis of both lung tissues and bronchoalveolar lavage. Normal values for leukocyte composition were determined via 16-color flow cytometry and then the same assay was used to evaluate the lung environment of rhesus macaques infected with Ebola virus and African Green monkeys that had been infected with Nipah virus via aerosol challenge.

LIST OF TABLES

Table		Page
1	Summary of phenotypes used to define leukocyte subsets	10
2	Cytometer configuration	11
3	Clones used in the panels	13

LIST OF FIGURES

Figure		Page
1	Comparison of lung data from rhesus macaques with previously published data	21
2	Comparison of bronchoalveolar lavage data from rhesus macaques with previously published data	22
3	Variability in results in lung from four collection sites in African Green monkeys	24
4	Leukocyte composition of uninfected African Green monkey lung	25
5	Leukocyte composition of uninfected African Green monkey bronchoalveolar lavage	27
6	Comparison of leukocyte composition in uninfected vs. Ebola-infected rhesus macaques	29
7	Comparison of Ki-67 expression in lung leukocytes of uninfected vs. Ebola-infected rhesus macaques	31
8	Detection of Ebola VP40 in lung leukocytes of rhesus macaques after aerosol challenge with Ebola	33
9	Comparison of lung leukocyte composition of uninfected and Nipah-infected African Green monkeys	35
10	Comparison of bronchalveolar leukocyte composition of uninfected and Nipah-infected African Green monkeys	37
11	Comparison of Ki-67 expression by lung leukocytes of	

	uninfected and Nipah-infected African Green monkeys	39
12	Comparison of Ki-67 expression by bronchoalveolar lavage leukocytes of uninfected and Nipah-infected African Green monkeys	40
13	Detection of Nipah antigen in lung leukocytes of Nipah-infected African Green monkeys	43
14	Detection of Nipah antigen in bronchoalveolar lavage leukocytes of Nipah-infected African Green monkeys	44

LIST OF ABBREVIATIONS

ABSL	Animal Biosafety Level
ACK	Ammonium-Chloride-Potassium
Ag	Antigen
AGM	African Green Monkey
AM	Alveolar Macrophages
APC	Allophycocyanin
APC-Cy7	Allophycocyanin- Cyanine 7
BAL	bronchoalveolar lavage
BD	Becton Dickinson
BV	Brilliant Violet
BSL	Biosafety level
CD	cluster of differentiation
EBOV	Ebola virus
FBS	Fetal Bovine Serum
FITC	Fluorescein isothiocyanate
FMO	Fluorescence Minus One
FSC-A	Forward Scatter Area

FSC-H	Forward Scatter Height
Gran	granulocytes
g	gravitational force
HLA	human leukocyte antigen
IM	interstitial macrophages
μm	micron
μL	microliter
mL	milliliter
min	minutes
mDC	myeloid dendritic cell
NK	natural killer cell
NHP	Nonhuman primate
NiV	Nipah virus
Perm	Permeabilization
PBS	Phosphate Buffered Saline
PE	Phycoerythrin
PerCP-Cy5.5	Peridinin Chlorophyll Protein Complex – Cyanine 5.5
pDC	plasmacytoid dendritic cell

RPMI	Roswell Park Memorial Institute
SSC-A	Side Scatter Area
SSC-H	Side Scatter Height
U	units

INTRODUCTION

Background

Outbreaks of highly infectious viral pathogens with high mortality rates occur occasionally throughout the world. Members of the filovirus and paramyxovirus families have been responsible for significant outbreaks within the last 20 years. Mortality rates vary with outbreaks and agents. According to the WHO, mortality rates from Ebola virus (EBOV) infection, the most well-known filovirus as well as the most recent significant outbreak in West Africa from 2014-2016 (CDC, 2018), have varied between 25-90% with an average of 50% (WHO, 2017). Outbreaks of the paramyoxovirus, Nipah virus (NiV) have had case fatality rates between 40-100% (Cong *et al.*, 2017). While these agents are not closely related phylogenetically, they do share some similarities in pathology and are included together in this work because the studies performed on these agents are similar in design, logistics, and goals. It is important to study these agents in controlled laboratory settings in order to understand the natural pathologies associated with them as well as to identify effective treatments and vaccines to treat and protect against them. A complete understanding of the pathology of each agent is necessary in order to identify possible targets for treatment. In addition to the threat of natural infection, there is also concern that some of these viruses, most notably the filoviruses, could be used as bioweapons. These viruses can only be studied in high containment Biosafety Level 4 (BSL-4) laboratories because of the high mortality rates associated with them, the lack of available treatments and vaccines against them, and because they are highly infectious (Kuhn *et al.*, 2011).

The amount of information that can be gleaned from in vitro viral studies is limited, so animal models are frequently used. As in many other areas of research, nonhuman

primate (NHP) models are frequently used in studies of BSL-4 viral pathogens because NHPs are genetically similar to humans. The selection of NHP species used in a study depends on similarities in disease course to that exhibited by infected humans as well as considerations stemming from the goals of the study (St Claire *et al.*, 2017). Various macaque species and African green monkeys (grivet monkeys) (AGM) are very commonly used in NHP studies.

The choice of viral challenge route, intravenous (IV), intramuscular (IM), intranasal (IN), intratracheal (IT) and aerosol challenge, can align with the pathogens suspected natural infection route or be based on which challenge route induces a pathology that is most similar to that observed in natural infections. Aerosol challenge involves introduction of aerosolized virus into the lungs of the animal that is being challenged (Reed *et al.*, 2011). Aerosol challenge may be used if there is concern that the agent could be aerosolized for use as a bioweapon (Twenhafel *et al*., 2013) or if aerosol is considered a natural route of exposure for the agent (Cong *et al.*, 2017).

Ebola virus infections occur after contact with bodily fluids from infected individuals or animals. The possibility of aerosol transmission of Ebola is controversial though EBOV antigen has been found in the nasal and airway surfaces of infected NHPs (Johnson *et al*., 1995) indicating that the tissues of the respiratory tract are susceptible to both infection and viral shedding and NHPs have been repeatedly shown to be susceptible to aerosol challenge (Mekibib and Arien, 2016). Nevertheless, no known cases of human infection via aerosol route have been reported. Concerns persist that EBOV could either naturally mutate or be purposely weaponized in some manner that could make it capable of aerosol transmission.

Nipah virus is thought to be transmissible via contact with fomites, consumption of contaminated foods, or close contact with infected individuals (Cong *et al*. 2017; Clayton, 2017). It has been shown that African Green monkeys (AGMs) can be infected with NiV via intratracheal or aerosol route in the laboratory (Cong *et al*., 2017; Johnston *et al*., 2015). Infection of both humans and AGMs is characterized by both respiratory and neurological disease (Cong *et al*., 2017). Like EBOV, no infection of a human via aerosol has been reported for NiV; however, its human-to-human transmissibility, high fatality rate, and lack of available treatments/vaccines make it a concern as a possible bioweapon.

Rationale

The lungs are a primary site of infection in aerosol challenge studies, so it is of interest to study changes in the lung environment after challenge. Unlike blood, lung can only be collected at necropsy. As a result, it is only possible to collect cross-sectional data on lung tissue as opposed to longitudinal data over the course of the study. This presents two complications. The first is that it is difficult to determine how the lung tissue has changed due to infection because there is no way to collect pre-challenge data. There is very little published data available about what types of cells can be detected in the lungs of NHP species or what the phenotypes of each cell type might be in this compartment. Therefore, in order to determine changes due to infection, the data was compared to normal control data collected from normal control monkeys. The second is that NHPs in BSL-4 studies are typically euthanized and necropsied either when they reach end-point criteria due to severe disease or at the conclusion of the study if the animal has survived and apparently recovered from infection. As a result, it is difficult to discern what was happening in the survivors while they were battling infection, which would be the best

comparison to the tissues collected from monkeys that were euthanized during acute disease.

Bronchoalveolar lavage (BAL) samples can be collected on live animals by injecting and then subsequently aspirating fluid from the lung via bronchoscope (Schultheiss *et al.*, 2011; Wolf and White, 2012). It is possible to collect (BAL) samples on live, anesthetized NHPs; therefore, BAL samples can be used to provide longitudinal information about the lung environment. However, the variety of leukocytes that are found in BAL samples is more limited than in whole lung tissue so data from this sample type does not provide as complete a picture as data from lung samples.

Since neither sample type is optimal in providing a complete picture of the lung environment during infection, both types of sample were collected. Samples were processed, stained with fluorochrome-conjugated antibodies and stains and characterized through the use of a flow cytometer. A single cell solution was created from samples collected from NHPs and then stained with fluorochrome-conjugated antibodies to both surface and intracellular proteins. After staining, samples were run through a cytometer to evaluate which of the proteins were present on or in each cell. The combination of proteins detected was used to determine cell type, detect proliferating cells (through the expression of cellular proliferation marker Ki-67), and look for viral antigen positivity through the use of antibodies to viral proteins that were labeled in-house with fluorochromes. The phenotypes of each leukocyte type were defined the same in both sample types since they exist within the same compartment. Therefore, the same panel was used for both tissue types.

There is very little published data available regarding what types of cells can be detected in the lungs of NHP species or what the phenotypes of each cell type might be in this compartment. It was considered reasonable to assume that the phenotypes of some cell types, such as B cells, T Cells, and Natural Killer cells would be the same as they are in whole blood. However, for other cell types such as macrophages, phenotype can vary with compartment, function, and activation state (Laskin *et al*., 2001 and Ortiz *et al*., 2015). Therefore, definitions that have been previously published (Cai *et al.*, 2014) for rhesus macaque lung macrophages were used for the rhesus samples and an attempt was made to apply these definitions to the AGM samples. African green monkeys have been shown to have high levels of sequence conservation with both humans and rhesus macaques (Warren *et al.*, 2015) so it was deemed a reasonable starting point to use the same designations as rhesus and use anti-human clones that are cross-reactive to construct the panel for the AGMs; however, the designations made in the paper did not apply well to AGMs because their lung macrophages appeared to lack expression of CD163 that was used to define macrophage types in the rhesus. However, differential expression of HLA-DR and CD11b were also explored in the Cai paper, and those definitions appeared to apply to the AGM samples. This difference in phenotypes across species was not unanticipated as it has been previously described in other compartments (Beaumier, 2009).

Rhesus macaques are the most commonly used model for Ebola virus studies (Bennett, 2017); whereas, Nipah virus studies use AGM because the disease course they exhibit closely resembles that of humans (Geisbert *et al*., 2010). In order to be able to identify changes in these tissues due to infection, lung and BAL samples from uninfected control monkeys were first collected and analyzed to be compared to those of the infected

NHPs that were subsequently collected. The data from the uninfected control macaques was compared to those published in the Cai paper in order to evaluate the effectiveness of our panel(s) in identifying the various leukocyte populations of interest (Cai *et al.*, 2014). The data from the infected monkeys was compared to those obtained using the same panels in uninfected NHP from the same species in order to identify changes that may be due to infection.

Studies conducted on NHPs in a BSL-4 environment are frequently done on small sample sizes because of the expense of conducting this type of work and because of the difficulties of working in a BSL-4. The small sample sizes that were used in the studies investigated here make it difficult to determine statistical significance; therefore, only basic trends can be observed as changes in the lung environment due to infection.

Most antibodies used in flow cytometry of NHP samples are anti-human antibodies that are cross-reactive with NHP species. Cross-reactivity was confirmed prior to use wherever possible either by screening on cells from each species or by search of published data in which the clone was used in each species and clones were selected that were cross-reactive with both NHP species where possible. Antibodies for proliferation and viral antigen detection were added to the panels in an attempt to identify populations that were expanding due to infection as well as those that were positive for viral antigen.

Objectives

The overall objective of these studies was to develop a flow cytometry assay to evaluate leukocyte composition of lung and BAL samples from rhesus macaques and AGM and

then use the panel to study changes in these species after aerosol challenge with Ebola virus and Nipah Virus, respectively.

Objective 1: Develop a Flow Cytometry Panel that Can be Used to Evaluate Leukocyte Composition of Normal Rhesus Macaque and AGM Lung and BAL Samples.

The panel contained stains for cellular proteins that allowed for the identification of the following leukocyte types: T Cells, B Cells, Natural Killer (NK) Cells, alveolar macrophages (AMs), interstitial macrophages (IMs), myeloid dendritic cells (mDCs), and plasmacytoid dendritic cells (pDCs). These stains were used to determine the leukocyte composition of the samples collected. In order to identify proliferating cells, Ki-67 intracellular stain was included in the panel. Stains for appropriate viral proteins were created in-house in attempt to identify cells that were positive for viral antigen.

Objective 2: Use the Panel that was Developed to Analyze Lung and BAL Samples from Uninfected Control NHP Tissues in Order to Determine Normal Reference Ranges for Each Species and Tissue Type.

At least two samples of each species and sample type were collected from uninfected animals (with the exception of rhesus BAL) and analyzed in order to define normal values. The data collected from the rhesus macaques was compared to published data (Cai *et al.*, 2014). Only one rhesus BAL sample was obtained for comparison to published data, but this was not considered a weakness, since BAL samples were not collected from infected rhesus.

Objective 3: Use the Panel to Look for Changes in Lung Tissue Collected from Rhesus Macaques Infected via Aerosol Route with Ebola Virus.

Lung samples were collected from NHP on an Ebola virus study and analyzed using the developed panel. Data were compared to reference ranges determined in Objective 2.

Objective 4: Use the Panel to Look for Changes in Lung Tissue and BAL Collected from AGM Infected via Aerosol Route with Nipah Virus.

Lung and BAL samples were collected from AGM on a NiV study and compared to the reference ranges determined in Objective 2.

MATERIALS AND METHODS

Panel Design

The rhesus panel was designed largely based on phenotypes described in published literature (Cai et al., 2014) as shown in Table 1. The available BD Fortessa cytometers (Becton Dickinson San Jose, CA) allowed for the discrimination of 16 colors simultaneously as described in Table 2. One color was reserved for a live/dead fixable viability dye that was used to gate out dead cells. One color was reserved to stain for a viral protein using antibodies labeled in-house. In an attempt to ascertain which cells were actively proliferating in the lung environment, one color was reserved for the cellular proliferation marker, Ki-67 (Scholzen and Gerdes, 2000).

Table 1. Summary of the phenotypes used to define each cell subset in the lung and BAL of rhesus macaques. These phenotypes were defined in a paper by Cai *et al.* (2014); wherein, they were used to define normal leukocyte composition of these tissues.

Cell Type	Phenotype
CD4+ T Cells	CD45+, Low Side Scatter, CD3+, CD4+
CD8+ T Cells	CD45+, Low Side Scatter, CD3+, CD8α+
B Cells	CD45+, Low Side Scatter, CD3-, CD4-, CD8α-, CD20+, HLA-DR+
Natural Killer Cells	CD45+, Low Side Scatter, CD3-, CD8α+
Granulocytes	CD45+, CD11b+, HLA-DR-
Myeloid Dendritic Cells	CD45+, HLA-DR+, CD163-, CD206-, CD11c+, CD123-
Plasmacytoid Dendritic Cells	CD45+, HLA-DR+, CD163-, CD206-, CD11c-, CD123+
Alveolar Macrophages	CD45+, HLA-DR+, CD163+, CD206+, CD11b+, HLA-DR++
Interstitial Macrophages	CD45+, HLA-DR+, CD163+, CD206-, CD11b++, HLA-DR+

Table 2. The cytometer configuration allowed for successful compensation of simultaneous staining in the colors shown in the table.

Laser	Stain
Blue	FITC
	PerCP-Cy5.5
Green	PE
	PE-TexasRed, PE-CF594, or PE/Dazzle 594
	PE-Cy5
	PE-Cy7
Red	APC
	AlexaFluor 700
	APC-Cy7
Violet	BV 421
	Aqua Viability Dye
	BV570
	BV605
	BV650
	BV711
	BV785 or BV786

The monoclonal antibody clones that were used, shown in Table 3, have all been previously shown to be cross-reactive in both rhesus and AGM or were tested for cross-reactivity in AGM peripheral blood monocytes so the same antibodies were appropriate for the AGM samples. All antibodies were titrated, in order to determine the optimum concentration to use, on PBMCs from the appropriate species. This also served to absolutely confirm that the clones were cross-reactive. The one exception to this was the clone 19.2 for which no information could be found regarding cross-reactivity with AGM CD206. Since CD206 is not widely expressed on peripheral blood macrophages, it was not possible in advance to confirm cross-reactivity. No clones could be found in the literature that were cross-reactive with AGM CD206, so the decision was made to use 19.2 and use differential expression levels of HLA-DR and CD11b to discriminate between alveolar and interstitial macrophages as described by Cai *et al.* (2014) in the event that clone 19.2 was not cross-reactive with AGM CD206.

Table 3. Clones used in the panel. The exact panel of antibody-fluorochrome conjugates used was consistent within each species but the combinations used for Rhesus were slightly different than those used for AGM.

Antigen	Clone	Manufacturer
CD3	SP34-2	Becton Dickinson
CD4	L200	Becton Dickinson
CD8	SK1	Becton Dickinson or Biolegend
CD11b	ICRF44	Becton Dickinson or Biolegend
CD11c	S-HCL-3	Becton Dickinson
CD14	M5E2	Becton Dickinson or Biolegend
CD16	3G8	Becton Dickinson or Biolegend
CD20	2H7	Becton Dickinson or Biolegend
CD45	D058-1283	Becton Dickinson
CD123	7G3	Becton Dickinson
CD163	GHI/61	Becton Dickinson
CD206	19.2	Becton Dickinson
HLA-DR	L243	Becton Dickinson or Biolegend
Ki-67	B56	Becton Dickinson

Tissue Collection

Where possible samples were collected from at least two normal control animals for each species and tissue type. This was possible for rhesus lung and both tissue types in AGM; however, only one BAL sample was collected for normal rhesus. Since BAL was not collected from EBOV-infected rhesus, the staining of this tissue type was largely to confirm that the panel created could attain similar results to those already published by Cai *et al*. (2014). One sample was adequate to achieve this goal. Since there is no published data about AGM lung leukocyte composition, four samples were collected from each control AGM, two from the left caudal region and two from the right cranial region of the lung, in order to assess differences in different regions of the lung in this species. Cai *et al.* (2014) had previously demonstrated that there was little difference in leukocyte composition in various regions of the lungs of rhesus macaques.

In the NiV study, two lung samples were collected from each monkey. One sample was collected from a region that appeared to have disease-related lesions and the other was collected from an area that did not appear to have lesions. Bronchoalveolar lavage samples were collected at euthanasia only for this study. A bronchoscope was used to inject and subsequently aspirate fluid from the lungs of each monkey at the time of necropsy.

Lung tissues were removed from NHPs at necropsy by the pathology team and placed in a 50-mL conical that contained 10 mL of Advanced RPMI 1640 (ThermoFisher, Waltham, MA) with 10% FBS.

Tissue Processing

All samples from NHP were processed inside a biosafety cabinet. Samples that were taken from NHP that were housed inside an ABSL-4 at the time of necropsy were processed in a BSL-4 lab. Samples from monkeys that were housed at ABSL-2 were processed in a BSL-2 lab.

Lung tissue needed to be digested and disassociated to obtain a single cell solution for flow cytometry staining. To that end each lung tissue piece was placed in a 100 μm filter that was set up in a petri dish and then cut into small pieces of less than 1 cm using forceps and scissors. The samples were then digested by addition of Collagenase D (100U/mL) and DNase I (100U/mL) in 40 mL of Advanced RPMI + 10% FBS followed by incubation at 37°C for 30 min. Following digestion, the flat end of a syringe plunger was used to dissociate the tissue by pushing it through the filter. The filter and any remaining tissue were discarded and the media containing the cells was collected from the petri dish, added to a 50-mL conical tube and centrifuged at 280 x g for 10 min. Red cells were lysed in the pelleted cells by re-suspension in 5 mL of ACK Lyse (Quality Biological, Gaithersburg, MD) followed by incubation for 5 min at room temperature. Cells were then washed by addition of 40 mL of Advanced RPMI with 10% FBS followed by centrifugation at 280 x g for 10 min. One additional wash was performed on the pelleted cells using 50 mL of Advanced RPMI with 10% FBS. Cells were then re-suspended in PBS to be counted. Five to 10 million cells were transferred to a 12 x 75 mm tube and pelleted for staining.

Since BAL samples were already in solution, they were simply pelleted, washed with PBS + 2% FBS, counted, and five to 10 million cells were transferred to a 12 x 75 mm tube for staining.

Staining for Flow Cytometry

Surface staining cocktails were made by adding fluorochrome-labeled antibodies and Aqua Live/Dead Fixable Cell stain (ThermoFisher, Waltham, MA) to PBS. One hundred microliters of surface stain was added to each tube. The samples were incubated for 20 min at room temperature protected from light. Samples were washed by addition of 4 mL of PBS with 2% FBS followed by centrifugation at 250 x g for 5 min. The supernatant was decanted, and the samples were re-suspended in 500 μL BD Cytofix/Cytoperm Solution (BD Biosciences, San Jose, CA) and incubated at room temperature for 30 min in order to fix and permeabilize the cells for intracellular staining. The samples were then spun at 550 x g for 5 min and washed once with 2 mL of 1X BD Perm/Wash Buffer (BD Biosciences, San Jose, CA). Intracellular staining cocktail was made by addition of fluorochrome-labeled antibodies into 1X BD Perm/Wash Buffer. Intracellular staining was performed overnight at 4° C in a volume of 100 μL. The following day the samples were washed by addition of 4 mL of 1X BD Perm/Wash Buffer followed by centrifugation at 550 x g for 5 min and re-suspended in 200 μL of 1X BD Perm/Wash Buffer. Samples were either acquired immediately on the cytometer or stored at 4° C until acquisition.

All samples were acquired on an 18-color BD LSRFortessa cytometer. Prior to acquisition, compensation was performed using anti-Mouse IgG compensation beads (Spherotech, Lake Forest, IL) and ArC Amine Reactive Beads (ThermoFisher, Waltham,

MA) as appropriate. BD FACSDiva software (BD Biosciences, San Jose, CA) was used to calculate and apply compensation values to the sample tubes.

Samples were acquired and FCS files were exported and analyzed using Flow Jo software (BD Biosciences, San Jose, CA)

Fluorescence Minus One Controls

Fluorescence minus one (FMO) controls were stained at least once for each sample type to be used as gating controls for analysis purposes. Each FMO tube contained all of the stains in the staining cocktails used minus one. For example, the FITC FMO tube contained all of the stains that the sample tubes were stained with except for the FITC stain. FMO controls were used to define negative populations for each color. Fluorescence minus one controls were stained in exactly the same manner described above for the samples.

anti-Nipah Rabbit Polyclonal Antibody Development, Purification, and Labeling

Purified Nipah virus (NiV) glycoprotein (protein name: 293 Free-Tet-NiV-SG Tet) was supplied by Dr. Chris Broder at the Uniformed Services University. Polyconal antibody was raised in rabbits against the protein by ThermoFisher. Polyclonal antibody was purified in house from the resulting rabbit serum using a commercially available Protein A Antibody Purification Kit following manufacturer's instructions (Abcam) and concentrated using a commercially available Antibody Concentration Kit following manufacturer's instructions (Abcam). Protein concentration was determined using a NanoDrop 8000 (ThermoFisher) and conjugation with PE was performed using a commercially available PE Conjugation Kit (Abcam). The labeled antibody was titrated for use in intracellular staining of NiV-infected VeroE6 cells prior to use.

Mouse anti-EBOV VP40 Antibody Labeling

Mouse anti-EBOV VP40 monoclonal antibody (clone AE11) was obtained from IBT Bioservices. The monoclonal antibody was labeled with PE using a commercially available PE Conjugation Kit (Abcam). Labeled antibody was titrated for use in intracellular staining of EBOV-infected VeroE6 cells prior to use in the panel.

Data Analysis

FCS files were exported from FACS DIVA software and imported into FlowJo version 9.9.6. Doublets were excluded by gating events on a FSC-A vs FSC-H plot and gating on the events with a linear relationship between the area and height measurements. The same strategy was then employed using a SSC-A vs. SSC-H plot in order to ensure that most doublets were excluded from the analysis. Dead cells were then removed from the remaining events using Aqua Viability Dye vs SSC-A plot and gating on the lower staining populations. After removal of doublets and dead cells, the CD45+ events were gated on in order to exclude any epithelial cells or debris that had not been already excluded.

RESULTS

Objective 1: Develop a Flow Cytometry Panel to Evaluate Leukocyte Composition of Normal Rhesus Macaque and AGM Lung and BAL Samples

In order to evaluate our ability to reproduce published data with our panel, the control rhesus data that we attained was compared to those described in the Cai *et al.* (2014) paper. We analyzed one sample each from the lungs of four rhesus macaques. Figure 1 is a comparison between our rhesus lung data and those published. We detected a slightly lower proportion of both macrophage types, and natural killer cells than found in the published data and more granulocytes.

Figure 2 below is a comparison between our rhesus BAL data and those published by Cai *et al.* (2014). In the Cai paper the granulocytes were further broken down into neutrophils and eosinophils. We did not use markers that would allow us to differentiate between the different types of granulocytes. Our designation of granulocytes should be understood to potentially include all three subsets of granulocytes (neutrophils, eosinophils, and basophils). Our data from rhesus BAL were very similar to the published data. No actual percentages were listed in the published data (Cai *et al.*, 2014) but, based on a visual interpretation of the provided figure, approximately 90% of the leukocytes identified were macrophages, approximately 10% were lymphocytes, and a very small percentage of granulocytes were identified. In our data, 86% of the leukocytes identified were macrophages, 11 Since the paper did not break down the macrophage or lymphocyte populations further, the plot in Figure 2 shows data only for macrophages, lymphocytes

(defined as the combined populations of B cells, T Cells, and NK cells), and granulocytes for an easier comparison to the data in the paper.

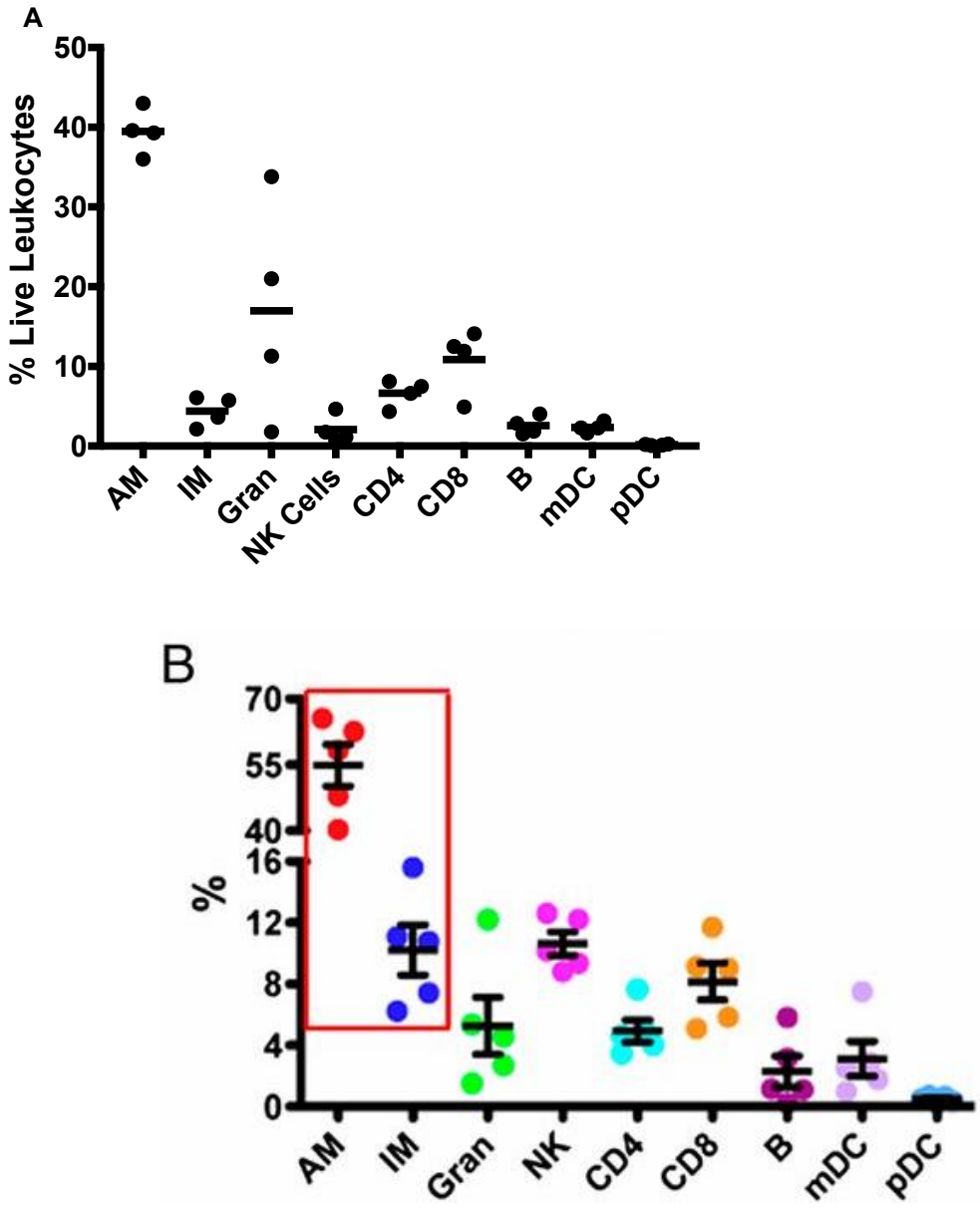

Figure 1. Comparison of data collected from uninfected rhesus monkey lung on this study with those published by Cai *et al*. (2014). The data in A is our data and B is the published data. Horizontal axes indicate the percentage of leukocytes that were found to be of each subset. Each dot represents the data from one monkey, bars represent the mean of all samples analyzed. Abbreviations: Alveolar Macrophages (AM), Interstitial Macrophages (IM), Granulocytes (Gran), Natural Killer Cells (NK), CD4+ T Cells (CD4), CD8+ T Cells (CD8), B Cells (B), myeloid dendritic cells (mDC), plasmacytoid dendritic cells (pDC)

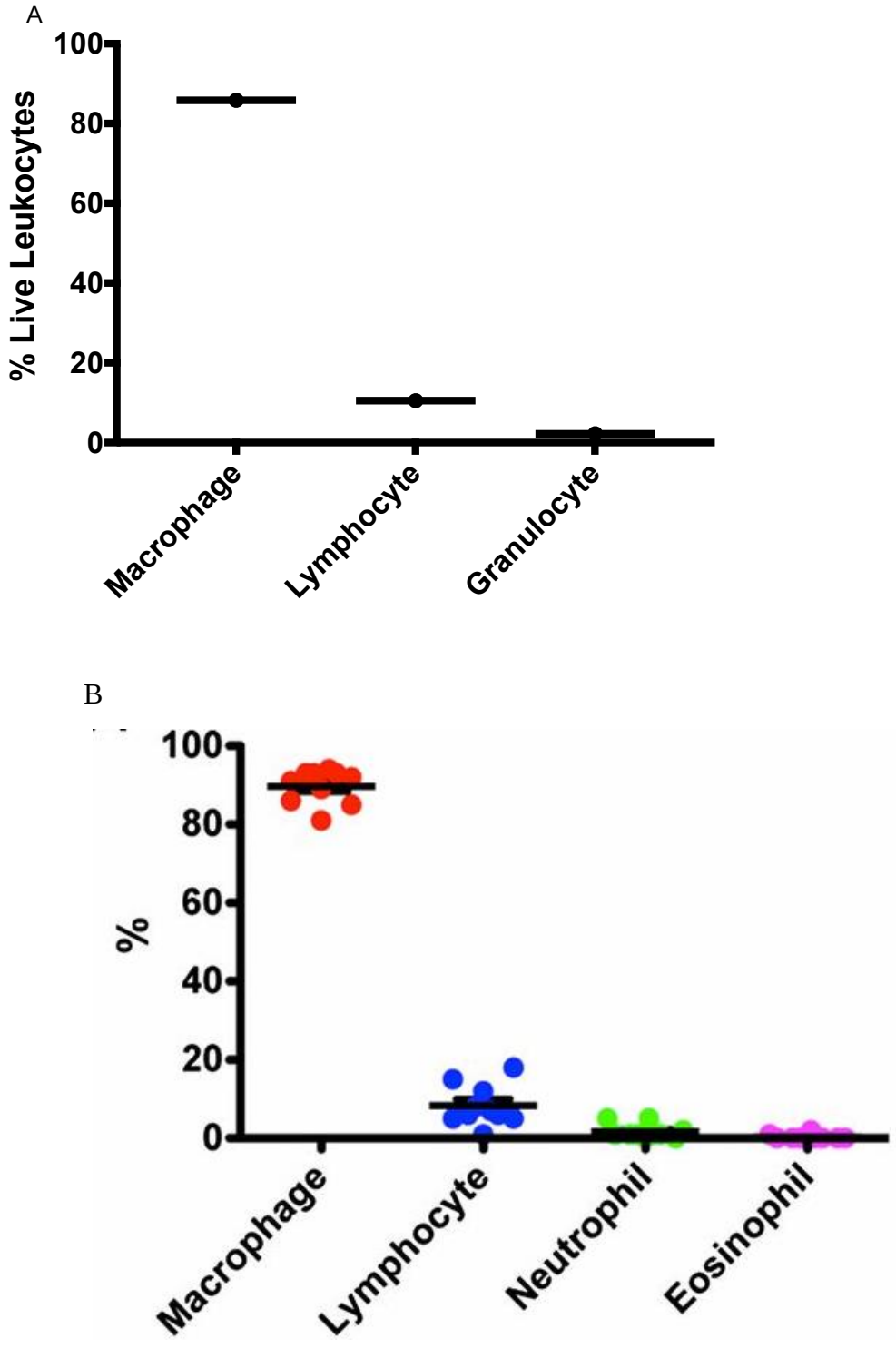

Figure 2. A comparison of the data acquired using our panel on Rhesus BAL with those published by Cai *et al.* (2014). The data in A is our data, the data in B is from the paper. Horizontal axes indicate the percentage of leukocytes that were found to be of each subset. Each dot represents the data from one monkey, bars represent the mean of all samples analyzed.

Objective 2: Use the Panel that was Developed to Analyze Lung and BAL Samples from Uninfected Control NHP Tissues in Order to Determine Normal Reference Ranges for Each Species and Tissue Type

The normal control data for the rhesus tissue types is shown above in Figures 1 and 2 (A). To determine if sample collection site was a factor, four samples were collected from each normal AGM from different sites in the lung. Figure 3 shows the results from the four samples along with the mean of each. The results of the four samples were fairly consistent within the samples collected from a given monkey. Figure 4 shows the data that was obtained from the staining of lung samples from uninfected AGMs. In comparison to the normal Rhesus lung data in Figure 1, AGM lung samples had a lower percentage of alveolar macrophages (mean of 30.3% of leukocytes versus 39.5% in rhesus), granulocytes (mean of 0.5% of leukocytes versus 17% in rhesus), CD4+ T cells (mean of 2.5% of leukocytes versus 6.6% in rhesus), and mDCs (none identified in AGM versus 2.3% of leukocytes in rhesus) and higher percentage of interstitial macrophages (mean of 7.8% of leukocytes versus 4.4% in rhesus), natural killer cells (mean of 6.6% of leukocytes versus 2.1% in rhesus) , CD8+ T cells (mean of 32.7% of leukocytes versus 10.9% in rhesus), B cells (mean of 6.7% of leukocytes versus 2.6% in rhesus), and pDCs (mean of 7.3% of leukocytes versus 0.2% in rhesus).

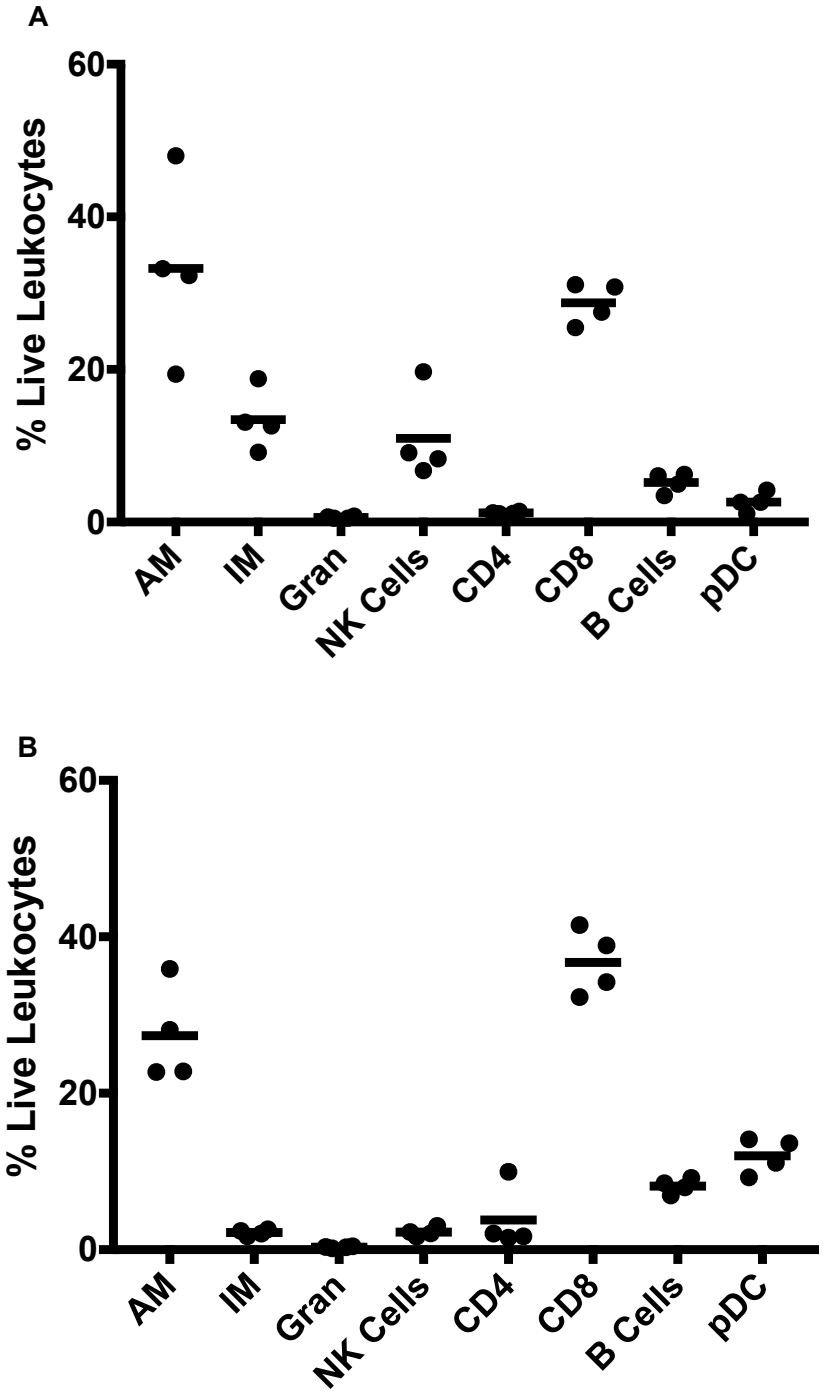

Figure 3 The variability in results across four samples collected from each control monkey. The data plotted in A is from monkey T612 and the data in B is from monkey T620. Each dot represents a different piece of tissue from the same monkey. Each bar represents the mean of the four samples collected from that monkey.

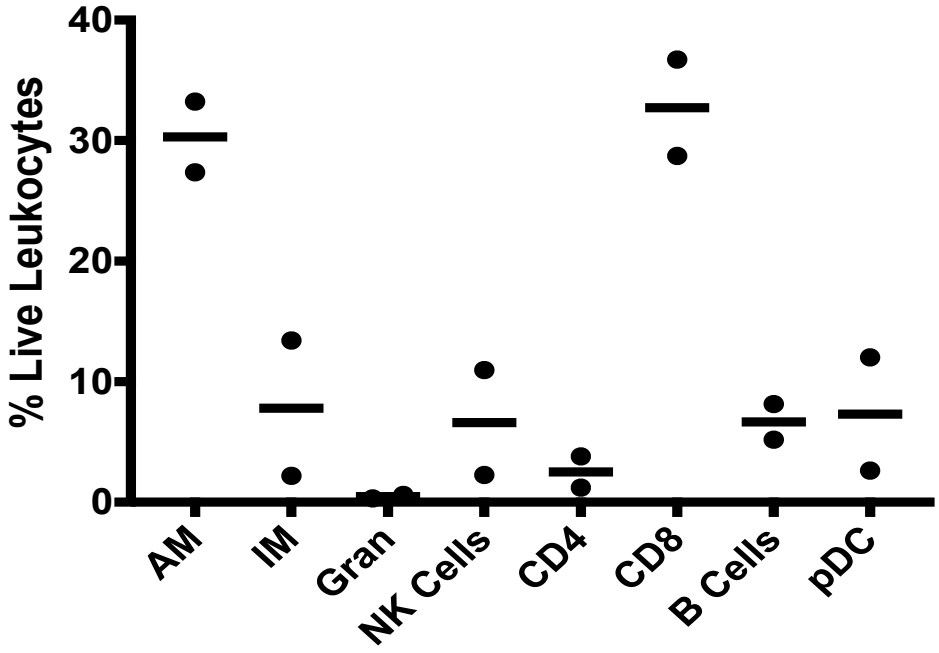

Figure 4 Data collected from the analysis of AGM lung samples. Each dot represents the average result of four samples per monkey. Each bar represents the mean of all samples collected.

Figure 5 shows data from the staining of BAL samples collected from uninfected AGMs. Though the CD163 clone used was shown to be cross-reactive with AGM CD163 through staining of AGM PBMCs, it did not appear to be expressed strongly on the surface of either lung macrophage subtype. Neither CD14 nor CD16 were expressed consistently on either macrophage type either so differential levels of HLA-DR and CD11b expression were used to designate alveolar and interstitial macrophages. Cai *et al.* (2014) previously correlated alveolar macrophages with higher levels of HLA-DR and slightly lower levels of CD11b and interstitial macrophages with higher levels of CD11b and slightly lower levels of HLA-DR. The percentage of mDCs found in AGM lungs was found to be negligible so they were not included in the data. In comparison to the BAL data from the uninfected rhesus sample as well as the published rhesus data (Cai *et al*., 2014), AGM BAL was found to contain a markedly higher percentage of lymphocytes (a mean of 29.6% of leukocytes versus 10.5% in rhesus) and lower percentage of macrophages than rhesus (a mean of 52.7% of leukocytes versus 85.9% in rhesus).

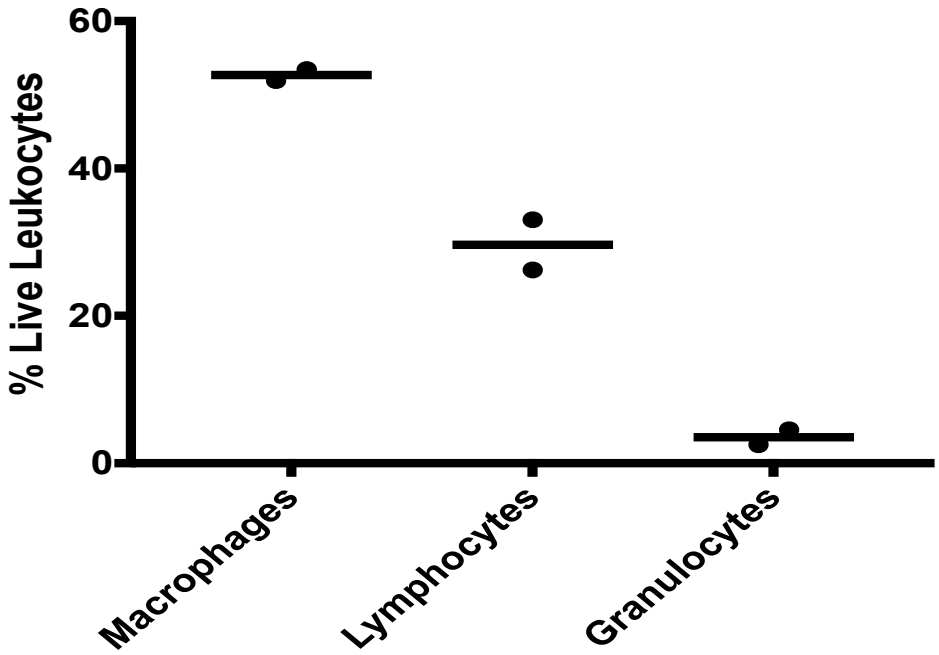

Figure 5 The data obtained from the staining of BAL samples from uninfected AGMs. Each dot represents the value from one sample (monkey). Each bar represents the mean of the two samples assayed.

Objective 3: Use the Panel to Look for Changes in Lung Tissue Collected from Rhesus Macaques Infected via Aerosol Route with Ebola Virus Compared to Our Control Rhesus Data

Samples were collected from 9 rhesus that had been exposed to aerosol challenge with EBOV. Two of the nine monkeys survived challenge and were euthanized at the end of the study after they had recovered from challenge. Since their lung samples were collected after recovery rather than at the peak of disease, the data from the two survivors was considered a third group. Figure 6 is a comparison of the lung composition data from the control rhesus lung samples. The samples from the rhesus that were euthanized due to severe illness are included in the non-survivors group, and those that survived are labeled survivors. The data presented is an average of the monkeys in each group. The uninfected group contained four monkeys, the non-survivors group contained seven monkeys, and the survivor group contained two monkeys. The number of monkeys per group is insufficient at this time to perform statistical analysis to determine statistical significance. Only basic trends can be observed for future investigations from this number of samples.

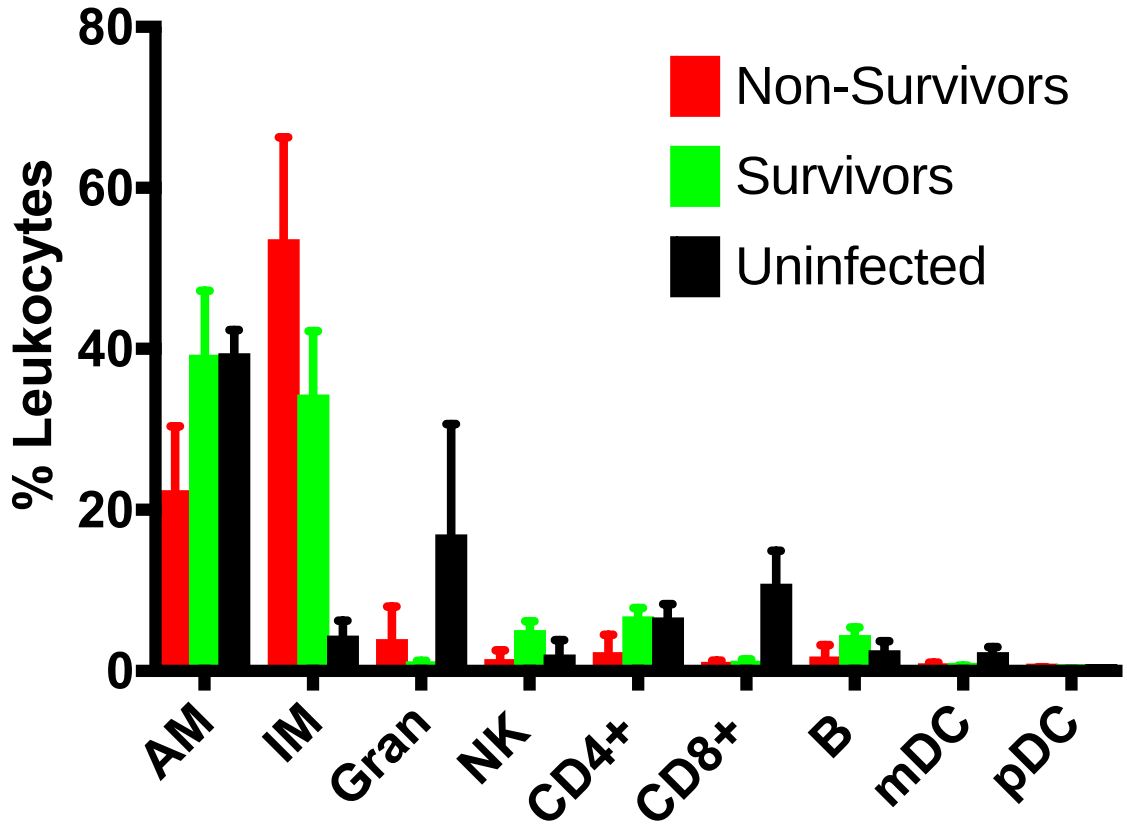

Figure 6 Comparison of leukocyte composition of Rhesus macaques that had been exposed via aerosol challenge to EBOV (separated into survivors and non-survivors) with the data attained from the normal control monkeys. Error bars indicate the standard deviation for each group/cell subset.

There were notable differences observed between the three groups. A dramatic increase in interstitial macrophages (a mean of 4.4% of leukocytes in the controls versus 53.6% in non-survivors and 34.3% in survivors) and decreases in CD8+ T Cells (a mean of 10.9% of leukocytes in the controls versus 0.7% in non-survivors and 1% in survivors) , myeloid dendritic cells (a mean of 2.3% of leukocytes in the controls versus 0.4% in non-survivors and 0.4% in survivors), and granulocytes (a mean of 17.0% of leukocytes in the controls versus 3.95% in non-survivors and 0.9% in survivors)was detected in both of the EBOV-infected rhesus groups relative to the uninfected control monkeys. The proportion of alveolar macrophages was markedly decreased in the monkeys that were euthanized at the peak of disease (a mean of 39.5% of leukocytes in the controls versus 22.4% in non-survivors); whereas, the monkeys that survived challenge had an increased proportion of natural killer cells (a mean of 2.1% of leukocytes in the controls versus 5.1% in survivors). Samples from the non-survivor group had a decrease in CD4+ T Cells at the time of euthanasia (mean of 2.3% of leukocytes in the controls versus 53.6% in non-survivors and 34.3% in survivors); whereas, the survivors had proportions of CD4+ T Cells that were similar to the uninfected controls (mean of 6.8% of leukocytes in the survivors and 6.6% in controls).

In order to ascertain which populations of cells were actively dividing, Ki-67 expression was measured in each population. The proportion of each population that was positive for Ki-67, and therefore actively dividing (Scholzen and Gerdes, 2000), is shown in Figure 7 below.

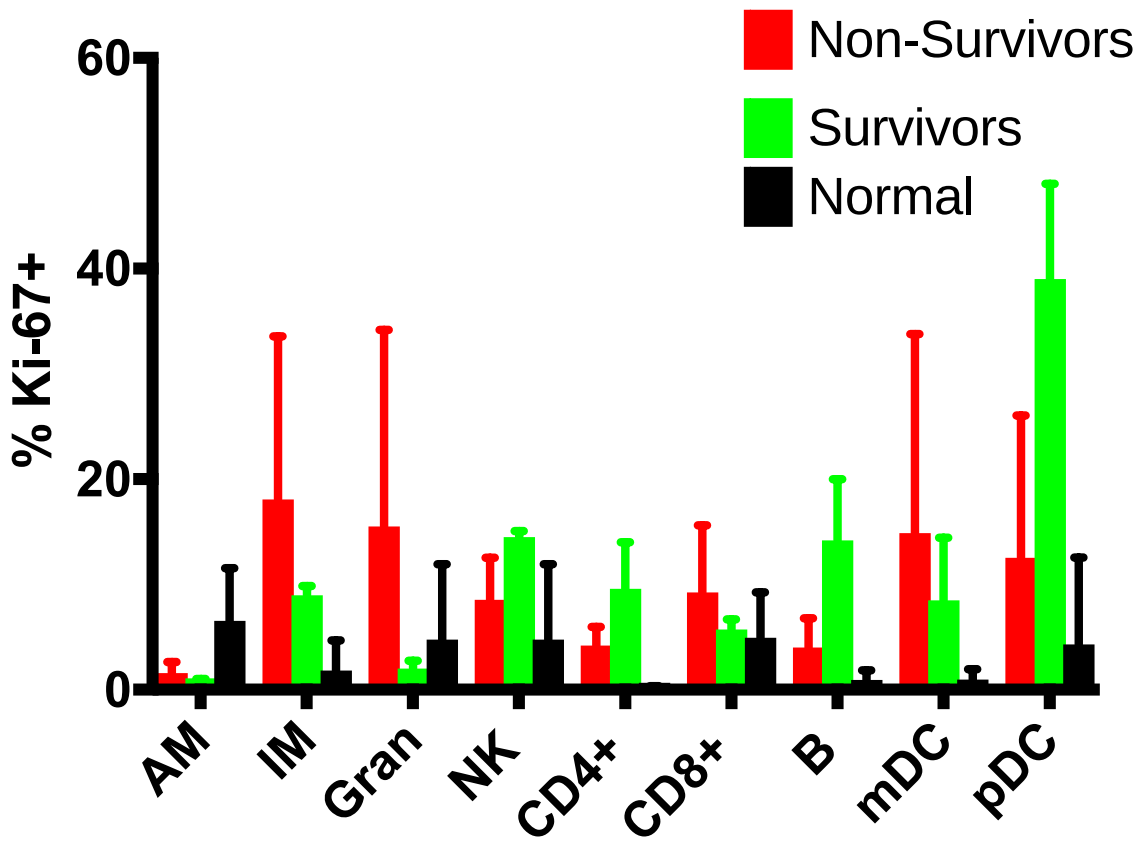

Figure 7 Expression of the cellular proliferation marker, Ki-67, in the lung leukocyte populations that were detected. Error bars indicate the standard deviation for each group/cell subset.

Most of the changes in Ki-67 expression levels relative to the uninfected controls were consistent between the non-survivors and survivors. All of the infected monkeys had lower levels of Ki-67 expression in their alveolar macrophages (a mean of 6.5% of leukocytes positive for Ki-67 in the controls versus 1.6% in non-survivors and 1% in survivors) and higher levels of Ki-67 expression in their interstitial macrophages (a mean of 1.8% of leukocytes positive for Ki-67 in the controls versus 18.0% in non-survivors and 9.0% in survivors), natural killer cells (a mean of 4.8% of leukocytes positive for Ki-67 in the controls versus 8.5% in non-survivors and 14.5% in survivors), CD4+ T Cells (a mean of 0.1% of leukocytes positive for Ki-67 in the controls versus 4.2% in non-survivors and 9.6% in survivors), B cells (a mean of 1.4% of leukocytes positive for Ki-67 in the controls versus 4% in non-survivors and 14.2% in survivors), and both dendritic cell types (a mean of 0.8% of leukocytes positive for Ki-67 in the controls versus 14.9% in non-survivors and 14.2% in survivors in mDCs and a mean of 4.3% of leukocytes positive for Ki-67 in the controls versus 12.5% in non-survivors and 39% in survivors in pDCs).

The percentage of each cell subset where EBOV VP40 could be detected is shown in Figure 8 below. All subsets of cells were found to be positive for viral antigen in the group that was euthanized at the peak of disease while marked decreases were observed at the time of necropsy in the survivors. Both dendritic cell subsets had a high percentage of antigen positive cells in the non-survivor group and viral antigen detection was also high in the pDCs of the survivors. A mean of 70.4% of non-survivor and 4.7% of survivor mDCs and 53.0% of non-survivor and 27.5% of survivor pDCs were found to be viral antigen positive.

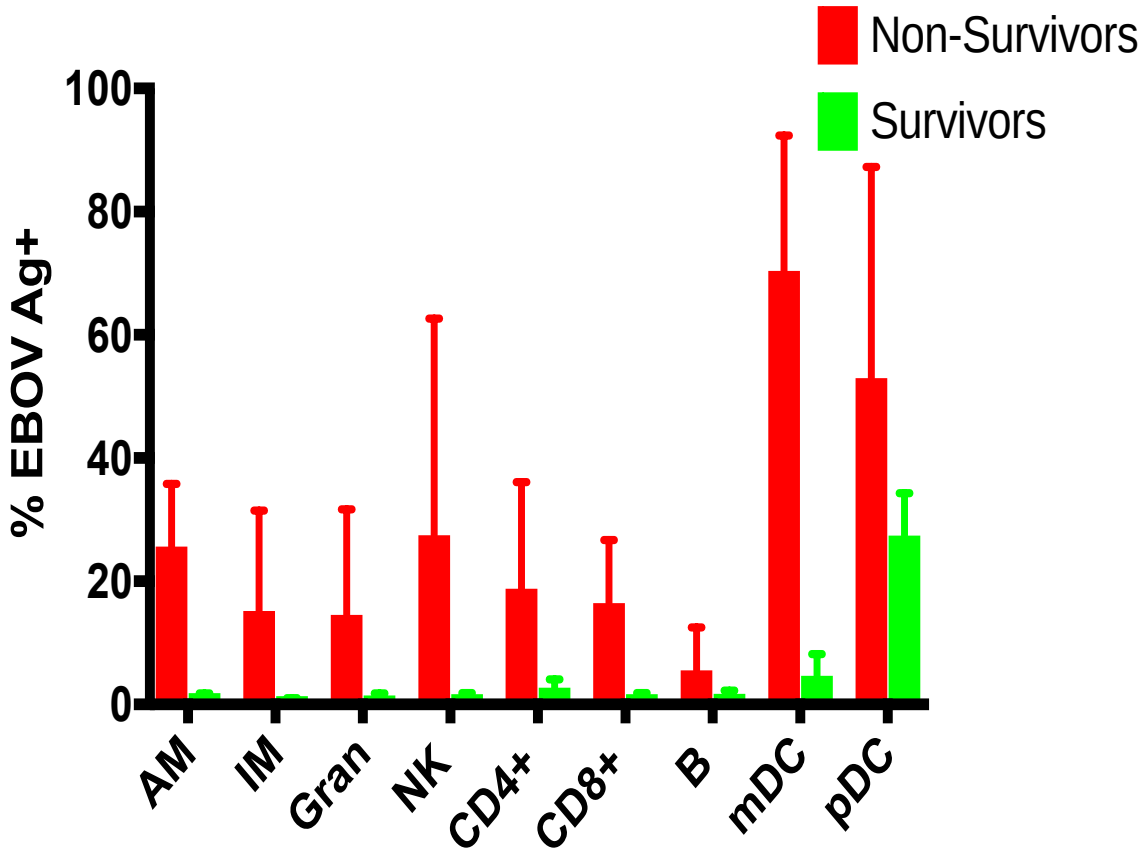

Figure 8 The percentage of each subset of cells in which EBOV VP40 could be detected in at the time of necropsy for the infected monkeys. Error bars indicate the standard deviation for each group/cell subset.

Objective 4: Use the Panel to Look for Changes in Lung Tissue and BAL Collected from AGM Infected via Aerosol Route with Nipah Virus

Two lung samples and one BAL sample were collected immediately following euthanasia from AGMs that had been challenged via aerosol route with NiV. One of the lung samples collected was from an area that appeared to have lesions due to disease, the other was collected from an area that did not appear to have lesions. The two sample types were very similar so an average of the data from the two samples was used rather than a comparison between them. Three monkeys were euthanized at the peak of disease because they had met end point criteria, meaning that they were deemed to be close to death from disease. One monkey survived and was euthanized at the conclusion of the study approximately 4 weeks after those that were euthanized at the peak of disease. Figure 9 below compares the leukocyte composition of the lung tissue in the non-survivors and survivor to the normal control animals. Myeloid dendritic cells were found in such small numbers in the AGM tissues that they were excluded from the analysis. As in the rhesus samples, the number of samples analyzed in this dataset is insufficient to perform statistical analyses. As a result, only observations of general trends that may be further investigated in future studies can be made.

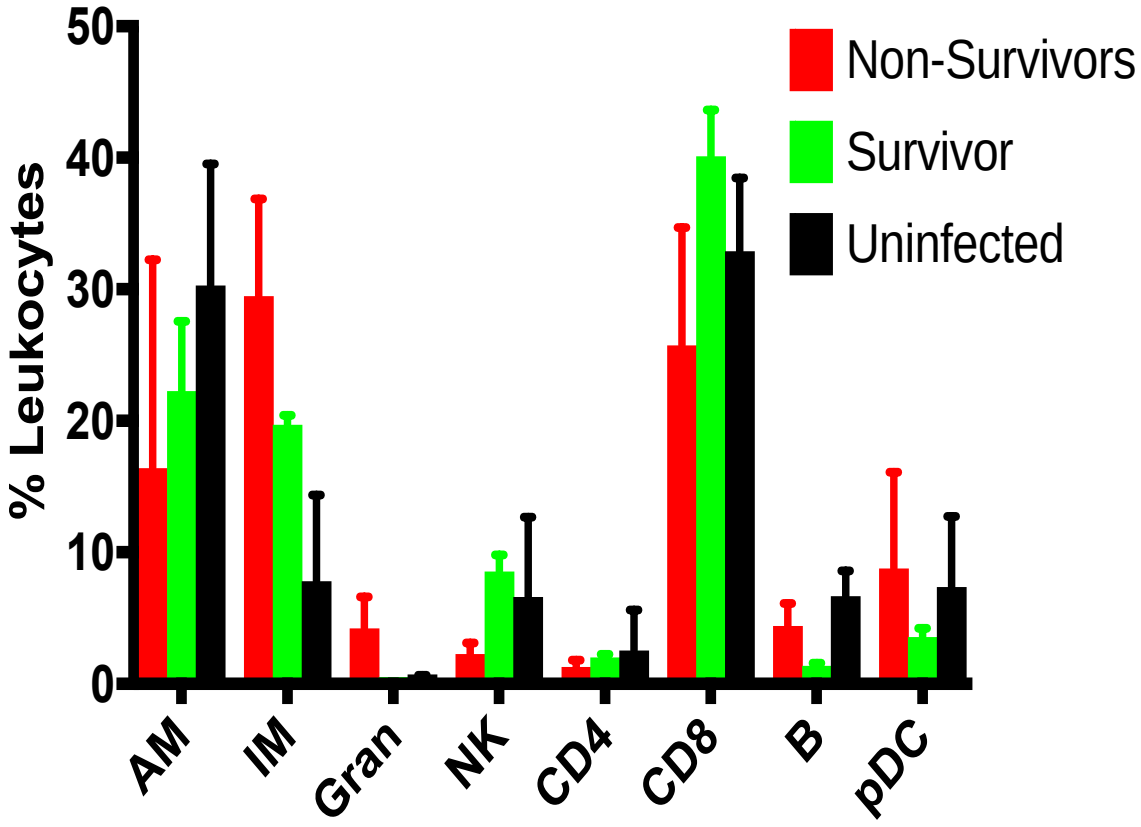

Figure 9 Comparison of the leukocyte composition in the lungs of AGMs that had been challenged via aerosol with Nipah virus, divided into survivors and non-survivors, to that of normal uninfected animals. Error bars indicate the standard deviation for each group/cell subset.

There was an increased percentage of interstitial macrophages (a mean of 7.8% of leukocytes in the controls versus 29.5% in non-survivors and 19.7% in the survivor) and decrease in alveolar macrophages (a mean of 30.3% of leukocytes in the controls versus 16.4% in non-survivors and 22.2% in survivors) for both of the challenged groups relative to the uninfected controls. The non-survivors had increased levels of granulocytes (a mean of 4.2% of leukocytes in the non-survivors versus 0.5% in the controls and 0.1% in the survivor) and decreased levels of natural killer cells relative to the other two groups (a mean of 2.3% of leukocytes in the non-survivors versus 6.6% in the controls and 8.5% in the survivor) and the survivor had increased levels of CD8+ T cells (a mean of 40.1% of leukocytes in the survivor versus 32.7% in the controls and 25.8% in the non-survivors) and decreased levels of B cells (a mean of 1.4% of leukocytes in the survivor versus 6.66% in the controls and 4.4% in the non-survivors) and plasmacytoid dendritic cells (a mean of 3.6% of leukocytes in the survivor versus 7.3% in the controls and 8.8% in the non-survivors) relative to the other two groups.

Figure 10 below shows a comparison of the BAL data in the different groups of AGM. There was a decrease in B cells in the non-survivor group (a mean of 2.2% of leukocytes in the non-survivors versus 6.7% in the controls and 9.78% in the survivor). The survivor that was euthanized after recovery from disease had an increased proportion of CD8+ T cells (a mean of 37.4% of leukocytes in the survivor versus 24.1% in the controls and 8.7% in the non-survivors) and B cells (a mean of 9.8% of leukocytes in the survivor versus 6.7% in the controls and 2.2% in the non-survivors) and a decreased proportion of granulocytes (a mean of 0.7% of leukocytes in the survivor versus 3.5% in the controls and 4.3% in the non-survivors).

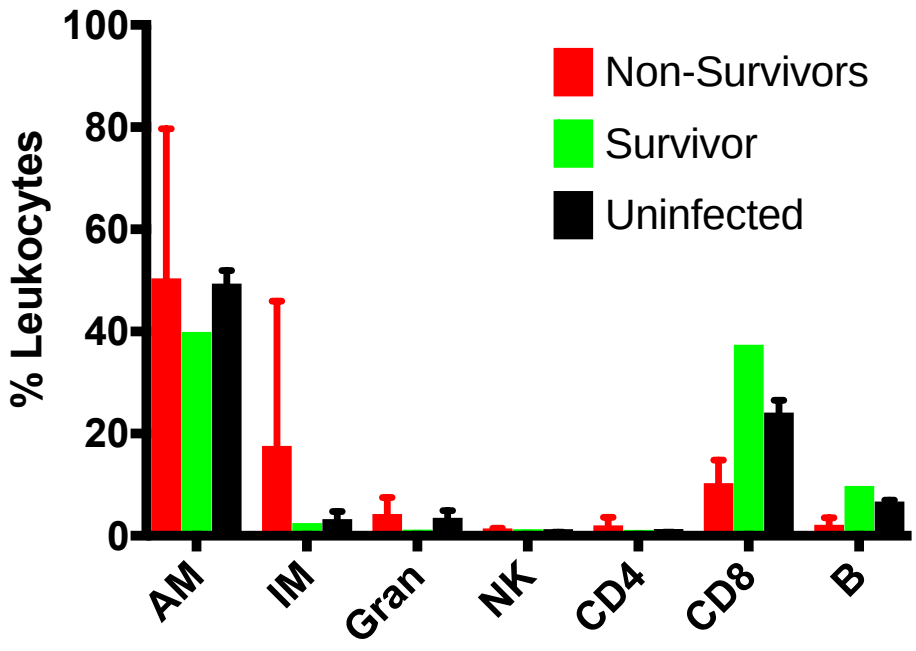

Figure 10 Comparison of BAL data from samples collected from AGM that were euthanized due to disease with the survivor and the normal controls. Error bars indicate the standard deviation for each group/cell subset.

As was performed in the rhesus sample, analysis of Ki-67 expression was determined in each subset in order to detect proliferating subsets. The results of the Ki-67 analysis of the AGM lung samples is summarized in Figure 11 and the BAL data is summarized in Figure 12.

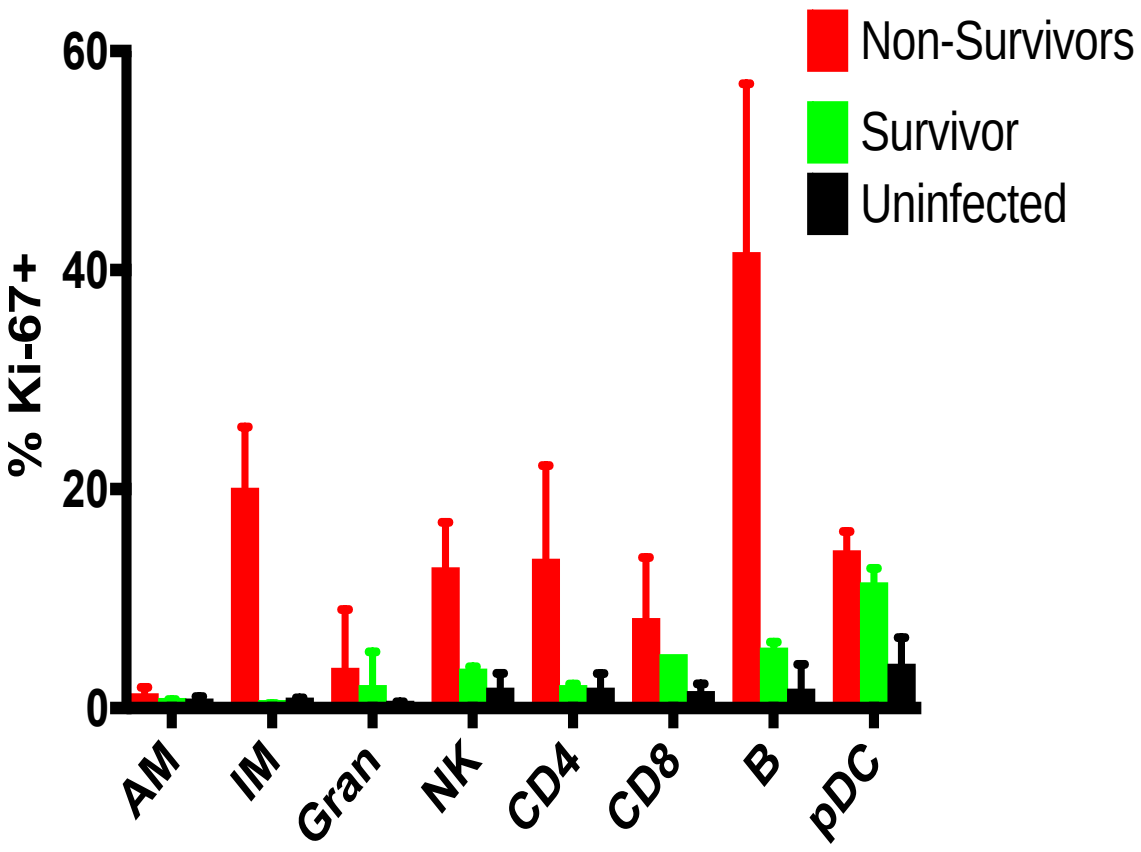

Figure 11 Comparison of the expression of the proliferation marker, Ki-67, in the lung samples collected from the NiV-challenged AGM with the normal uninfected control monkeys. Error bars indicate the standard deviation for each group/cell subset.

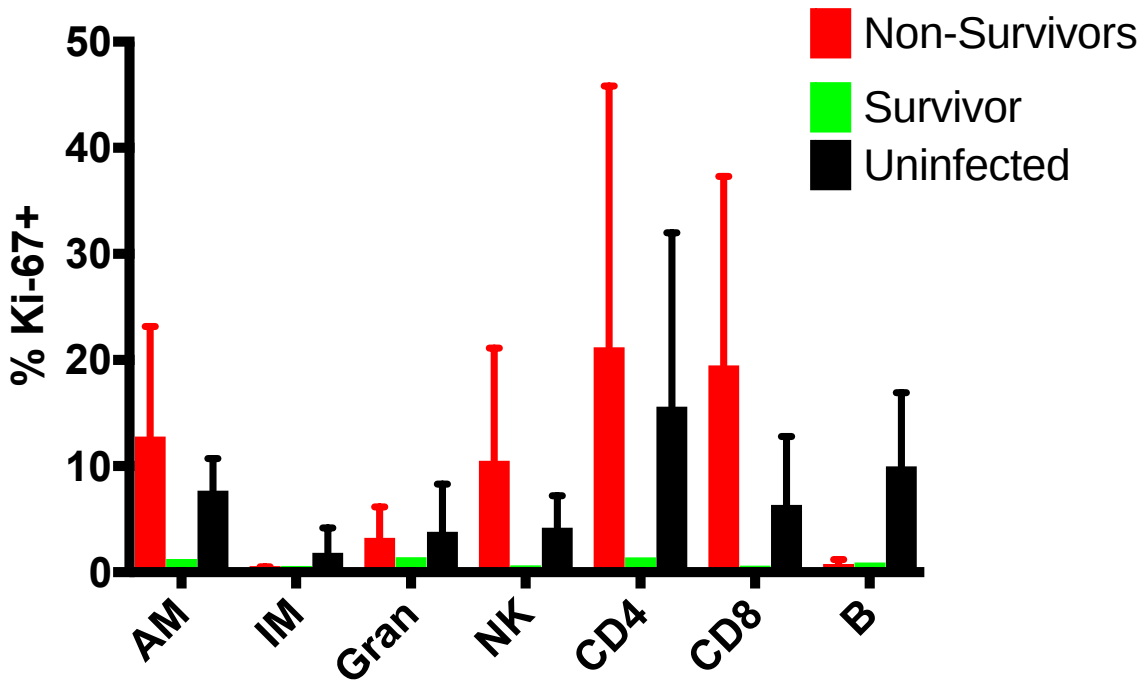

Figure 12 Comparison of Ki-67 expression in the BAL samples of both groups of NiV-challenged AGM with the uninfected controls. Error bars indicate the standard deviation for each group/cell subset.

An increase in Ki-67+ expression indicative of cell proliferation was detected in the lung granulocytes (a mean of 2.1% of granulocytes stained positive for Ki-67 in the survivor and 3.7% in the non-survivors versus 0.2% in the controls) and plasmacytoid dendritic cells (a mean of 11.5% of granulocytes were positive for Ki-67 in the survivor and 14.4% in the non-survivors versus 4.1% in the controls) of both challenged groups. The animals that were euthanized at the peak of infection, labeled the non-survivors, also had increased proliferation in interstitial macrophages (a mean of 20.1% of interstitial macrophages were positive for Ki-67 in the non-survivors versus 0.3% in the survivor and 0.8% in the controls), natural killer cells (a mean of 12.8% of natural killer cells were positive for Ki-67 in the non-survivors versus 7.2% in the survivor and 1.9% in the controls), CD4+ T cells (a mean of 13.7% of CD4+ T cells were positive for Ki-67 in the non-survivors versus 4.2% in the survivor and 1.9% in the controls), CD8+ T cells (a mean of 8.2% of CD8+ T cells were positive for Ki-67 in the non-survivors versus 4.9% in the survivor and 1.6% in the controls), and B Cells (a mean of 41.6% of B cells were positive for Ki-67 in the non-survivors versus 5.5% in the survivor and 1.8% in the controls).

In the BAL samples, an increase in Ki-67 expression was detected in the CD8+ T cells of the non-survivors (a mean of 19.5% of CD8+ T cells were positive for Ki-67 in the non-survivors versus 0.3% in the survivor and 6.3% in the controls). The levels of Ki-67 expression detected in the leukocytes of the BAL sample that was collected from the survivor were very low for all subsets.

The AGM samples that were collected from the NiV-challenged animals were also stained for Nipah antigen. Figures 13 and 14 depict the data from the lung and BAL samples respectively. Nipah antigen was detected in appreciable amounts in the lung granulocytes and plasmacytoid dendritic cells of the survivor (means of 21.5% of the granulocytes and 17.2% of pDCS in survivor samples stained positive for viral antigen) but only at very low levels in the non-survivors across all subsets. In contrast, most of the Nipah antigen detected in the BAL samples was found in the alveolar macrophages of the non-survivors (a mean of 13.1% of the alveolar macrophages in non-survivor samples stained positive for viral antigen) with very little being detected in any of the subsets of the survivor sample.

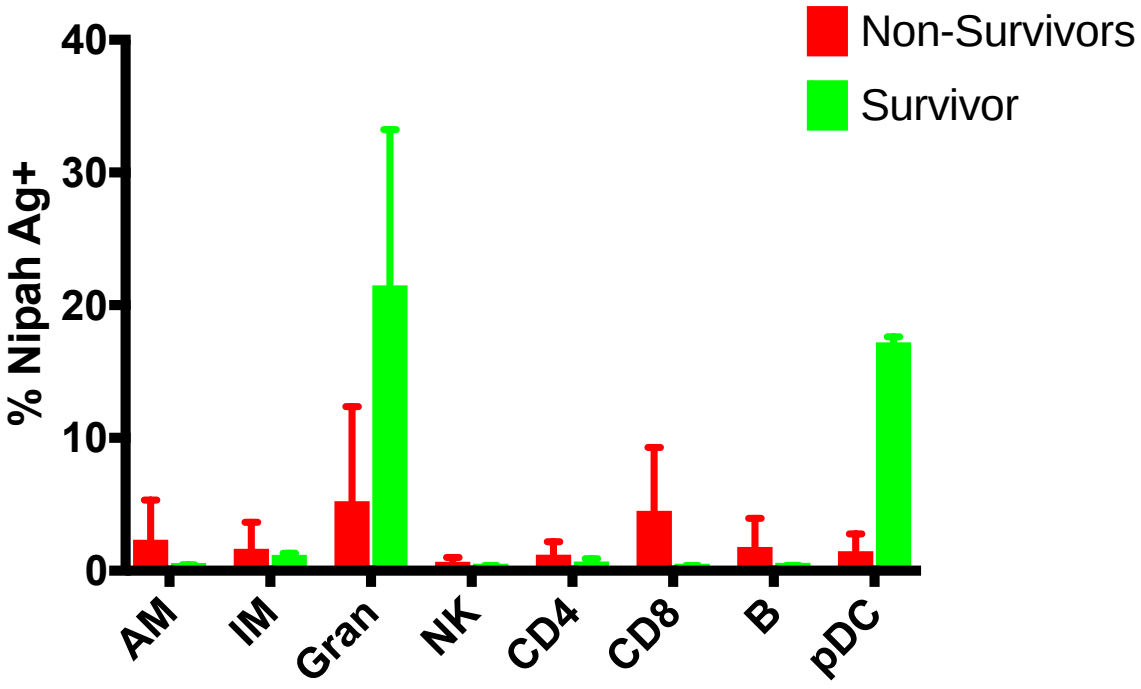

Figure 13 Detection of NiV antigen in the lung leukocytes of the two NiV-challenged AGM groups. Error bars indicate the standard deviation for each group/cell subset.

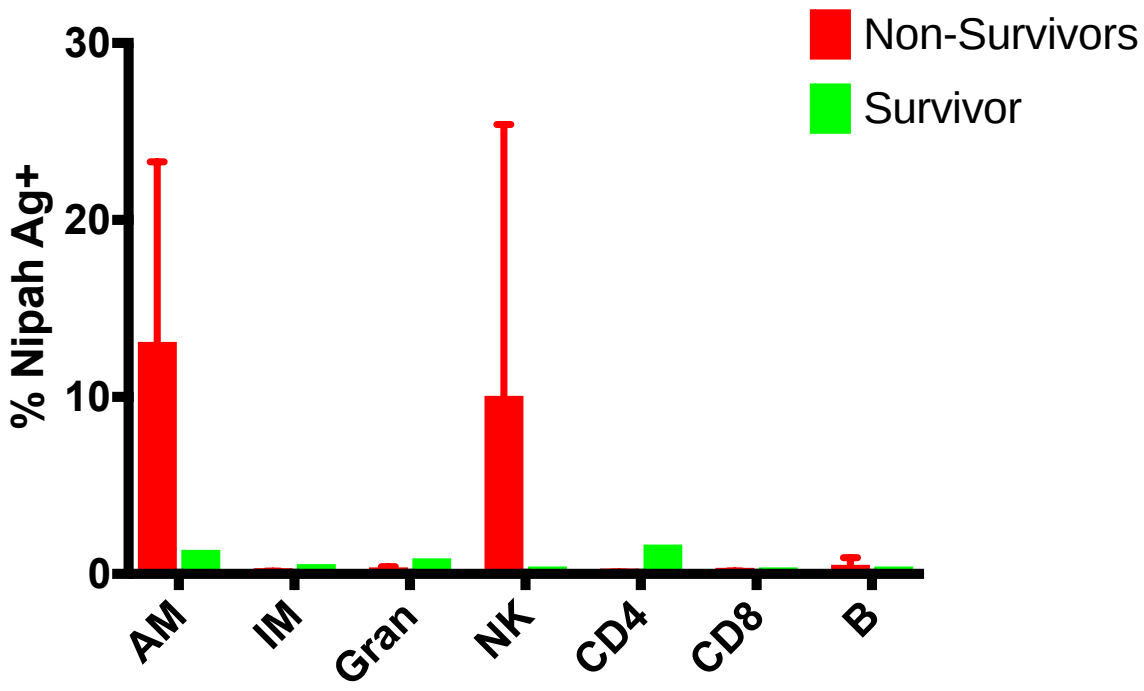

Figure 14 Results of the staining of BAL from NiV-challenged AGM samples for NiV antigen. Error bars indicate the standard deviation for each group/cell subset.

DISCUSSION

Objective 1: Develop a Flow Cytometry Panel that Can be Used to Evaluate Leukocyte Composition of Normal Rhesus Macaque and AGM Lung and BAL Samples

The panel of stains that was used in this work distinguished cell types rhesus macaque samples and compared well to previously published data (Cai *et al.*, 2014) with few exceptions. Most notably our data detected higher proportions of granulocytes and some lymphocyte types and lower proportions of macrophages than in the published data.

The number of samples (n) that were collected to confirm that our panel yielded similar results to those published by Cai *et al.* (2014) may have been insufficient. With only four lung samples being collected from normal rhesus, one outlier would skew our results more than it would with a higher sample number. Our results for granulocyte proportions had a higher variability than the other subsets identified, and one monkey did have a very high result that would have skewed our average towards higher granulocyte proportions. More samples will be collected in order to increase our n value and thereby get more reliable results.

It is also noteworthy that the three rhesus included in the normal control group, had the highest proportion of granulocytes in their lungs, were of an advanced age. It is very possible that there could be age-related changes in lung composition as well as other major organ systems. Some of these have previously been described by Simmons (2016). At least one of the factors described could lead to an increase in eosinophils in the lung which were included in the granulocyte category in this study. In the future, it would

probably be useful to make sure that the control monkeys used are of approximately the same age as those included in the study.

It is also possible that the increased proportions of granulocytes and lymphocytes in our normal samples was the result of some blood contamination. Granulocytes and lymphocytes make up a very high proportion of the leukocytes found in whole blood (Lee *et al.*, 2012). If the collection procedures used in this work resulted in higher levels of whole blood in the samples, it could explain the differences that were observed. Because the lungs serve to oxygenate the body's blood, there is always blood passing through them that could be included in the samples that were collected. Bronchoalveolar lavage samples can contain blood because the collection of the samples can cause minor amounts of irritation to the lung tissue that results in blood being present in the aspirate. Leukocytes that are contributed by whole blood contamination should be excluded from the analysis if at all possible since variability in amounts of whole blood contamination is a confounding factor.

Recently a method of injecting a primate with a labeled anti-CD45 antibody prior to euthanasia and then staining samples attained after euthanasia with an anti-CD45 antibody labeled with a different label in order to differentiate leukocytes that were contributed by whole blood from those that are resident to the tissue of interest was described by Wu *et al.* (2018). Incorporation of this technique would allow for the exclusion of whole blood leukocytes and remove this confounding factor from future studies. The leukocytes contributed by whole blood would be double positive for both stains; whereas, those that were resident to the tissue would not have the label that was injected into the bloodstream prior to euthanasia.

Objective 2: Use the Panel that was Developed to Analyze Lung and BAL Samples from Uninfected Control NHP Tissues in Order to Determine Normal Reference Ranges for Each Species and Tissue Type

The normal reference ranges that were determined for each species and sample type seem plausible and compare well, with few exceptions, to those previously published (Cai *et al*., 2014). In addition to being useful in measuring changes at the challenge site for aerosol challenges, these reference ranges could be useful in a variety of other areas of research as both rhesus macaques and AGMs have been used as models for various conditions and infections that affect the lungs. For example, rhesus have been used as models for tuberculosis (Kaushal *et al*., 2012) and influenza (Jegaskanda *et al*., 2013) while AGMs have been used as models for respiratory syncytial virus (Taylor, 2017) and pneumonic plague (Layton *et al*., 2011). These are all infections in which it might be of interest to monitor changes in the lung and BAL due to infection.

The most dramatic differences between the normal data from the two species were in lymphocyte and macrophage proportions with AGMs having a much higher proportion of lymphocytes and lower proportion of macrophages than rhesus in both tissue types. There were also species-specific differences in macrophage phenotypes.

It appears from these data that AGMs have a much higher proportion of lymphocytes in both tissue types than rhesus. Additionally, the proportion of lymphocytes that are CD8+ is higher in both tissue types in AGM than in rhesus. While no explanation for the increased proportion of lymphocytes in AGM is apparent at this time, the increased proportion of T cells that are CD8+ has been previously explained. Beaumier *et al*. (2009) described the downregulation of CD4 and upregulation of CD8α, as was used for the

staining panel in this work, in the memory CD4 cells of AGM. These cells that arise from CD4+ naïve cells retain many of the functions of CD4+ T cells in spite of the lack of expression of CD4 on their surface. While they dimly express CD8α, they express it in a CD8α/α homodimer as opposed to the CD8α/β heterodimers that are typically expressed on conventional CD8+ T cells. Vinton *et al*. (2017) further found that these CD8α dim cells account for the majority of T cells in AGM BAL which seems to agree with our data. It may have been possible to differentiate between conventional CD8+ T cells and formerly CD4+ T cells that are dimly expressing CD8α by gating on dim and bright CD8α+ cells, but that was not attempted in these analyses. Discriminating between the two would be made easier by the addition of a stain for CD8β to future iterations of the AGM panel as the conventional CD8+ T cells would be double positive for CD8α and CD8β, while the memory CD4 cells would be positive for CD8α but negative for CD8β.

Additional markers would also be helpful in discriminating between alveolar and interstitial macrophages in the AGM tissues. As previously mentioned, CD163 did not appear to be expressed on the lung and BAL macrophages of AGM. In the absence of CD163 expression to define the macrophage types, differential levels of CD11b and HLA-DR expression were used as described in rhesus by Cai *et al.* (2014) and in humans by Bharat *et al*. (2016). Cai *et al* showed that CD68 could be used in a similar manner to CD163 for rhesus and Bharat *et al.* found that CD169 was expressed on human alveolar macrophages but not on human interstitial macrophages. In future iterations of the AGM panel it would be potentially useful to add CD68 and CD169 if cross-reactive clones could be found in order to see if either of those markers could be used to delineate the macrophage subsets.

Objective 3: Use the Panel to Look for Changes in Lung Tissue Collected from Rhesus Macaques Infected via Aerosol Route with Ebola Virus Compared to Our Control Rhesus Data

There were some marked differences found in leukocyte composition, proliferation, and Ag-positive frequencies of the EBOV-infected rhesus relative to the uninfected controls. Some of the observed changes were similar between the two infected groups and some were not. It is reasonable to assume that some of the differences between the infected groups are due to tissue collection at the peak of disease rather than after apparent recovery from disease; however, there is no way, at this time, to know what data from the surviving monkeys would have looked like at the peak of disease.

The most dramatic of these differences was an increase in interstitial macrophages that was accompanied by an increase in detection of Ki-67 in this subset of cells in both groups of infected monkeys. There is far less published information about interstitial macrophages relative to alveolar macrophages largely because alveolar macrophages are relatively easy to collect from live individuals by bronchoalveolar lavage; whereas, isolation of interstitial macrophages requires lung biopsy and disassociation of the retrieved tissue by enzymatic digestion (Schyns *et al.*, 2018; Liegeois *et al.*, 2018). They were initially viewed as an intermediate state between blood monocytes and alveolar macrophages; however, recent research has indicated that the two macrophage phenotypes have distinct lineages and different functions (Schyns *et al.*, 2018). The idea of macrophages that proliferate in situ in the lung is somewhat controversial. Publications can be found that maintain that neither lung macrophage type self-renews in situ, instead both are replenished by an influx of blood monocytes that differentiate either sequentially

into interstitial macrophages and then alveolar macrophages (Landsman and Jung, 2007) or directly from monocyte to one macrophage type or the other (Cai *et al.*, 2014). Other publications make a case for self-replenishing macrophages in the lung that are capable of in situ proliferation (Hashimoto *et al.*, 2013; Landsman and Jung, 2007). We postulate that either, as has been shown to be possible (Hashimoto *et al.*, 2013; Landsman and Jung, 2007), the interstitial macrophages that we detected were in fact proliferating, or an influx of proliferating blood monocytes that are in the process of becoming interstitial macrophages was detected. Interstitial macrophages have been found to provide an anti-inflammatory role in the lung environment (Kawano *et al.*, 2016; Liegeois *et al.*, 2018; Cai *et al.*, 2014) and to be involved in antigen presentation to dendritic cells (Kawano *et al.*, 2014). In mice, they have also been shown to increase in response to hypoxic conditions (Liegeois e*t al.*, 2018). It is reasonable to postulate that the increase in interstitial macrophages demonstrates an attempt to control the initial inflammation that occurred as a result of infection. It is also possible that the infected monkeys experienced some level of hypoxia due to inflammatory effects of infection. Both imaging and multiplex cytokine data were collected, though not presented here, for these monkeys while on study. It would be interesting to correlate increase in anti-inflammatory cytokines as well as lung congestion detected in the imaging data with increases in interstitial macrophages of the infected monkeys. Both the differences in interstitial macrophage frequency and the increase in Ki-67 expression were more dramatic in the non-survivor group with the survivors exhibiting a less dramatic increase. This could be indicative of an increase in this subset during infection that then would, given enough time, return to baseline levels.

Unlike interstitial macrophages, no increase in alveolar macrophages was observed for either of the infected NHP groups. Alveolar macrophages are involved in phagocytosis and clearance of particulates from the alveolar spaces; whereas, interstitial macrophages are involved in controlling inflammation and antigen presentation (Cai *et al*., 2014). It makes sense that a macrophage type that is involved in both anti-inflammatory functions and antigen presentation would proliferate at the site of infection and inflammation but there would not necessarily be a need for an increase in a cell type that is involved in phagocytosis of particles.

While no increases in frequencies of either dendritic cell types were observed in either of the infected groups, there was an increase in Ki-67 expression in both dendritic cell subsets and both had high levels of Ag-positive cells. It is important to note that the presence of antigen does not imply infection of the cells. The cells could be infected, or they could have picked up antigen through phagocytosis. Dendritic cells sample antigens and then travel to the surrounding lymph nodes in order to present the antigens to naïve T cells that form responses to the antigens (Kopf *et al.*, 2015). The trends identified in this data are consistent with dendritic cells proliferating due to inflammation as indicated by the Ki-67 data, taking up antigen as indicated by the EBOV VP40 stain data, and then leaving the lung as indicated by the lack of increase in frequency of these cell types present in the lung. It would be interesting to try to track the dendritic cells to the draining lymph nodes in subsequent studies to see if there is an increase in dendritic cell frequencies in the lymph nodes as would be expected based on this data.

Objective 4: Use the Panel to Look for Changes in Lung Tissue and BAL Collected from AGM Infected via Aerosol Route with Nipah Virus

Several of the changes detected in the lung and BAL samples from NiV-infected AGMs could point to interesting avenues of investigation. Some, like the increase of interstitial macrophages in the lung of both infected groups, were more dramatic in the non-survivor group with a result in the survivor that was intermediate to the survivor and the uninfected controls, could be suggestive of an effect of acute infection that is returning to baseline in the survivor. Others, like the increase in CD8+ T cells in the lung of the survivor but not the non-survivors could be suggestive of the development of a protective response.

As was found in the lung and BAL of EBOV-infected Rhesus, there was an increase in interstitial macrophages in the lungs of both NiV-infected groups. As stated above, an increase in interstitial macrophages in the lung could be indicative of an anti-inflammatory response or possibly the result of the animal having experienced hypoxic conditions (Liegeois *et al*., 2018). Again, it would be interest to look for a corresponding increase in anti-inflammatory cytokines in the lung at the time of necropsy or increase in damage to lung tissue as determined by imaging data. Both multiplex cytokine data and imaging data are available for this study, though not presented here.

Perhaps even more interesting, is the increase in CD8+ T cells in the lung of the survivor at the time of necropsy. Gilchuk *et al*. (2016) described the presence of CD8 specific T cells in the lung interstitium of mice that had been vaccinated intranasally against vaccinia virus that conferred immunity. It would be very interesting to explore whether or not the increase in CD8 T cells in the lung of the surviving monkey could confer protective

immunity. There are several ways that this could be explored. If feasible, surviving animals could be maintained in the ABSL-4 until they have completely recovered from disease and then re-challenged via aerosol route to see if they exhibit a less acute disease course and recovery again. Alternatively, it may be possible to isolate CD8+ T cells from the lungs of survivors either through the use of magnetic bead isolation kits or using a cell sorter and then perform functional assays on them. An in vitro assay to look for production of the cytokines, Interferon gamma and Tumor Necrosis Factor alpha, in response to viral peptides could then be performed using in vitro stimulation with a Nipah peptide pool. This type of assay is very commonly performed to identify peptide-specific CD8+ T cells in the periphery of nonhuman primates that have been infected with various viruses (Donaldson *et al*., 2012). Less conclusive but more easily attained data could be gathered by simply adding the naïve and memory markers CD28 and CD95 to the lung panel. This would enable confirmation that the additional CD8+ T cells have a memory phenotype that could be further suggestive of a protective memory response. This approach would be more easily accomplished but there would be no way of conclusively stating that the cells were specific for Nipah virus.

Conclusions

Overall, the primary objectives of this study were accomplished. Additional improvements can be made in future studies to ensure that the data is as accurate as possible, and a few panel changes should be made in order to explore new avenues of interest as indicated by the data collected.

Since aerosol challenge of NHP is a commonly used strategy in the study of BSL-4 agents, it is important to understand what is happening at the challenge site both in order

to monitor disease progression and in order to identify possible targets for prevention of infection or treatment after infection at the challenge site. This data set could also be expanded to other nonhuman primate species such as cynomolgus monkeys and other viruses of interest in the future. The utility of this data is not limited to studies involving aerosol challenge with BSL-4 agents. The panels created could be applied to any number of NHP models. As stated above NHP are used as models for various respiratory diseases such as tuberculosis (Kaushal *et al*., 2012), influenza (Jegaskanda *et al*., 2013), respiratory syncytial virus (Taylor, 2017) and pneumonic plague (Layton *et al*., 2011). In all of these cases it would be useful to monitor changes in the lung since they are all respiratory illnesses.

None of the groups described in this work had a large enough sample size to allow for statistical analyses to determine statistical significance. It is very difficult to run large enough groups to allow for these types of analyses in NHP studies in a BSL-4 environment. The expense of running these types of studies as well as the logistical challenges of working in a BSL-4 laboratory mean that studies of this nature typically have very small sample sizes. No commentary can be made about the statistical significance of the data, only observations of general trends that can be further investigated in future studies. In particular the NiV model is still in the developmental stages. After a determination of what species, challenge route, and challenge dose is well established, larger sample sizes can be acquired by running several studies of smaller sample sizes and looking at the data as one larger data set. In spite of the small sample sizes for the Nipah study, the data from this study as well as the control AGM data was recently published (Hammoud *et al.*, 2018).

REFERENCES

Beaumier C, Harris L, Goldstein S, Klatt N, Whitted S, McGinty J, Apetrei C, Pandrea I, Hirsch V, Brenchley J. 2009. Down-regulation of CD4 by memory CD4+ T cells in vivo renders African green monkeys resistant to progressive SIVagm infection. Nat Med 15(8): 879-885.

Bennett R, Huzella L, Jahrling P, Bollinger L, Olinger G, Hensley L. 2017. Nonhuman primate models of Ebola Virus Disease. Curr Top Microbiol Immunol 411: 171-193.

Bharat A, Bhorade S, Morales-Nebreda L, McQuattie-Pimental A, Soberanes S, Ridge K, DeCamp M, Mestan K, Perlman H, Budinger G, Misharin A. 2016. Flow cytometry reveals similarities between lung macrophages in humans and mice. Am J Repir Cell Mol Biol 54(1): 147-149.

Cai Y, Sugimoto C, Arainga M, Alvarez X, Didier ES, Kuroda MJ. 2014. In vivo characterization of alveolar and interstitial lung macrophages in rhesus macaques: implications for understanding lung disease in humans. J Immunol 192(6): 2821-2829.

Centers for Disease Control and Prevention. 2018. Ebola Outbreaks 2000-2017 [Internet]. Atlanta(GA); [cited 2018 May 14] Available at: https://www.cdc.gov/vhf/ebola/outbreaks/history/summaries.html.

Clayton, B. 2017. Nipah virus: transmission of a zoonotic paramyxovirus. Curr Opin Virol 22: 97-104.

Cong Y, Lentz M, Lara A, Alexander I, Bartos C, Bohannon J, Hommoud D, Huzella L, Jahrling P, Janosko K, Jett C, Kollins E, Lackemeyer M, Mollura D, Ragland D, Rojas O, Solomon J, Xu Z, Munster V, Holbrook M. 2017. Loss in lung volume and changes in the immune response demonstrate disease progression in African green monkeys infected by small-particle aerosol and intratracheal exposure to Nipah virus. PLoS Negl Trop Dis 11(4):

Donaldson M, Kao S, Eslamizar L, Gee C, Koopman G, Lifton M, Schmitz J, Sylwester A, Wilson A, Hawkins N, Self S, Roederer M, Foulds K. 2012. Optimization and qualification of an 8-color intracellular cytokine assay for quantifying T cell responses in rhesus macaques for pre-clinical vaccine studies. J Immunol Methods 386 (1-2): 10-21.

Geisbert T, Daddario-DiCaprio K, Hickey A, Smith M, Chan Y, Wang L, Mattapallil J, Geisbert J, Bossart K, Broder C. 2010. Development of an acute and highly pathogenic nonhuman primate model of Nipah Virus infection. PLoS One 5(5): e10690.

Gilchuk P, Hill T, Guy C, McMaster S, Boyd K, Rabacal W, Lu P, Shyr Y, Kohlmeier J, Sebzda E, Green D, Joyce S. 2016. A distinct lung-interstitium-resident CD8(+) T cell subset confers enhanced protection to lower respiratory tract infection. Cell Rep 16(7): 1800-9.

Hammoud DA, Lentz MR, Lara A, Bohannon JK, Feuerstein I, Huzella L, Jahrling PB, Lackemeyer M, Laux J, Rojas O, Sayre P, Solomon J, Cong Y, Munster V, Holbrook MR. 2018. Aerosol exposure to intermediate size Nipah Virus particles induces

neurological disease in African green monkeys. PLoS Negl Trop Dis 12(11): e0006978. https://doi.org/10.1371/journal.pntd.0006978.

Hashimoto D, Chow A, Noizat C, Teo P, Beasley MB, Leboeuf M, Becker CD, See P, Price J, Lucas D, Greter M, Mortha A, Boyer SW, Forsberg EC, Tanaka M, van Rooiien N, Garcia-Sastre A, Stanley ER, Ginhoux F, Frenette PS, Merad M. 2013. Tissue-resident macrophages self-maintain locally throughout adult life with minimal contribution from circulating monocytes. Immunity 38(4): 792-804.

Jegaskanda S, Weinfurter J, Friedrich T, Kent S. 2013. Antibody-dependent cellular cytotoxicity is associated with control of pandemic H1N1 influenza virus infection of macaques. J Virol 87(10): 5512-5522.

Johnson E, Jaax N, White J, Jahrling P. 1995. Lethal experimental infections of rhesus monkeys by aerosolized Ebola virus. Int. J Exp Pathol 76(4): 227-236.

Johnston S, Briese T, Bell T, Pratt W, Shamblin J, Esham H, Donnelly G, Johnson J, Hensley L, Lipkin W, Honko A. 2015. Detailed analysis of African green monkey model of Nipah virus disease. PLoS One 10(2): e0117817.

Kaushal D, Mehra S, Didier P, Lackner A. 2012. The nonhuman primate model of tuberculosis. J Med Primatol 41(3): 191-201.

Kawano H, Kayama H, Nakama T, Hashimoto T, Umemoto E, Takeda K. 2016. IL-10-producing lung interstitial macrophages prevent neutrophilic asthma. Int Immunol 28(10): 489-501.

Kopf M, Schneider C, Samuel P. 2015. The development and function of lung-resident macrophages and dendritic cells. Nature Immunol 16: 36-44.

Kuhn J, Dodd L, Wahl-Jensen V, Radoshitzky S, Bavari S, Jahrling P. 2011. Evaluation of perceived threat differences posed by filovirus variants. Biosecur Bioterror 9(4): 361-371.

Landsman L, Jung S. 2007. Lung macrophages serve as obligatory intermediate between blood monocytes and alveolar macrophages. J Immunol 179(6): 3488-3494.

Laskin D, Weinberger B, Laskin J. 2001. Functional heterogeneity in liver and lung macrophages. J Leukoc Biol 70(2): 163-170.

Layton R, Brasel T, Gigliotti A, Barr E, Storch S, Myers L, Hobbs C, Koster F. 2011. Primary pneumonic plague in the African Green monkey as a model for treatment efficacy evaluation. J Med Primatol 40(1): 6-17.

Lee J, Shin J, Lee J, Jung W, Lee G, Kim M, Park C, Kim S. 2012. Reference values of hematology, chemistry, electrolytes, blood gas, coagulation time, and urinalysis in the Chinese rhesus macaques (*macaca mulatta*). Xenotransplantation 19(4): 244-8.

Liegeois M, Legrand C, Desmet C, Marichal T, Bureau F. 2018. The interstitial macrophage: A long-neglected piece in the puzzle of lung immunity. Cell Immunol https://doi.org/10.1016/j.cellimm.2018.02.001.

Mekibib, B and Arien, K. 2016. Aerosol transmission of filoviruses. Viruses 8(5): 148.

Reed D, Lackemeyer M, Garza N, Sullivan L, Nichols D. 2011. Aerosol exposure to Zaire ebolavirus in three nonhuman primate species: difference in disease course and clinical pathology. Microbes Infect. 13(11): 930-936.

Scholzen T and Gerdes J. 2000. The Ki-67 protein from the known and the unknown. J Cell Physiol. 182: 311-322.

Schultheiss T, Stolte-Leeb N, Sopper S, Stahl-Hennig C. 2011. Flow cytometric characterization of the lymphocyte composition in a variety of mucosal tissues in healthy rhesus macaques. J Med Primatol 40(1): 41-51.

Schyns J, Bureau F, Marichal T. 2018. Lung Interstitial Macrophages: Past, Present, and Future. J Immunol Res https://doi.org/10.1155/2018/5160794.

Simmons H. 2016. Age-associated pathology in rhesus macaques (macaca mulatta). Vet Pathol 53(2): 399-416,

St Claire M, Ragland D, Bollinger L, Jahrling P. 2017. Animal models of Ebolavirus infection. Comp Med 67(3): 253-262.

Taylor G. 2017. Animal models of respiratory syncytial virus infection. Vaccine 35(3): 469-480.

Twenhafel N, Mattix M, Johnson J, Robinson C, Pratt W, Cashman K, Wahl-Jensen V, Terry C, Olinger G, Hensley L, Honko A. 2013. Pathology of experimental aerosol Zaire ebolavirus infection in rhesus macaques. Vet Pathol 50(3): 514-529.

Vinton C, Ortiz A, Calantone N, Mudd J, Deleage C, Morcock D, Whitted S, Estes J, Hirsch V, Brenchley J. 2017. Cytotoxic T cell functions accumulate when CD4 is downregulated by CD4+ T cells in African Green Monkeys. J Immunol 198(1): 4403- 4412.

Warren WC, Jasinska AJ, Garcia-Perez R, Svardal H, Tomlinson C, Rocchi M, Archidiacono N, Capozzi O, Minx P, Montague MJ, Kyung K, Hillier LW, Kremitzki M, Graves T, Chiang C, Hughes J, Tran N, Huang Y, Ramesky V, Choi OW, Jung YJ, Schmit CA, Juretic N, Wasserscheid J, Turner TR, Wiseman RW, Tuscher JJ, Karl JA Schmitz JE, Zahn R, O'Connor DH, Redmond E, Nisbett A, Jacquelin B, Muller-Trutwin MC, Brenchley JM, Dione M, Antonio M, Schroth GP, Kaplan JR, Jorgensen MJ, Thomas GW, Han MW, Raney BJ, Aken B, Nag R, Schmitz J, Churakov G, Noll A, Stanyon R, Webb D, Thibaud-Nissen F, Nordborg M, Marques-Bonet T, Dewar K, Weinstock GM, Wilson RK, Freimer NB. 2015. The genome of the vervet (Chlorocebus aethiops sabaeus). Genome Res 25(12): 1921-33.

Weatherman S, Feldmann H, de Wit E. 2017. Transmission of henipaviruses. Curr Opin Virol 28: 7-11.

Wolf R, White G. 2012. Nonhuman Primates in Biomedical Research. 2nd ed. Cambridge (MA): Academic Press. Chapter 13, Clinical Techniques used for Nonhuman Primates; p 331.

Wong K, Shieh W, Kumar S, Norain K, Abdullah W, Guarner J, Goldsmith C, Chua K, Lam S, Tan C, Goh K, Chong H, Jusoh R, Rollin P, Ksiazek T, Zaki S. 2002. Nipah virus infection: pathology and pathogenesis of an emerging paramyxoviral zoonosis. Am J Pathol 161(6): 2153-2167.

World Health Organization. 2017. Ebola virus disease fact sheet [Internet]. Geneva (CH); [cited 2018 Jan 15]. Available at: http://www.who.int/mediacentre/factsheets/fs103/en/.

Wu C, Espinoza D, Koelle S, Potter L, Lu R, Li B, Yang D, Fan X, Donahue R, Roederer M, Dunbar C. 2018. Geographic clonal tracking in macaques provides insights into HSPC migration and differentiation. J Exp Med 215(1): 217-232.